Electronically Excited States and Their Role in Affecting Thermodynamic and Transport Properties of Thermal Plasmas

M. Capitelli, D. Bruno, G. Colonna, C. Catalfamo and A. Laricchiuta
Dept Chemistry University of Bari, via Orabona 4, 70125 Bari Italy
CNR IMIP Bari, via Amendola 122/D, 70125 Bari

mario.capitelli@ba.imip.cnr.it

ABSTRACT

The contribution of internal degrees of freedom to thermal-plasma properties has been investigated in a wide range of temperature and pressure.

Thermodynamic functions have been calculated modelling in different ways the electronic levels of atomic species (ground-state, Debye-Hückel and confined-atom approximations). Frozen and reactive specific heats are strongly affected by electronic excitation whereas compensation effects smooth its influence on the total specific heat, i.e. the sum of frozen and reactive contributions.

High-order Chapman-Enskog method has been applied to evaluate transport coefficients. The inclusion of electronically excited states have a twofold impact, reflecting the changes on thermodynamic properties and on transport cross sections of excited species.

Results for atomic hydrogen, nitrogen and air plasmas are considered in this lecture.

CONTENTS

INTRODUCTION **2**
PART I : THERMODYNAMIC PROPERTIES **3**
1.1 HYDROGEN PLASMAS 4
1.1.1 Method of calculation 4
1.1.2 Thermodynamic properties 7
1.1.3 Isentropic coefficients 11
1.2 NITROGEN PLASMAS 13
1.2.1 Thermodynamic properties 13
1.2.2 Isentropic coefficients 19
PART II : TRANSPORT PROPERTIES **21**
2.1 HYDROGEN PLASMAS 21
2.1.1 Cut-off of the atomic partition function 21
2.1.2 Collision integrals of electronically excited states 22
2.1.3 Transport properties 23
2.1.3.1 Influence of composition and thermodynamic properties 23
2.1.3.2 Influence of EES cross sections 26
2.2 AIR PLASMAS 30
2.2.1 Collision integrals for low-lying excited state 30
2.2.1.1 Resonant excitation/charge exchange processes 31
2.2.2 Transport properties 32
CONCLUDING REMARKS **36**
APPENDIX A TRANSPORT OF INTERNAL AND REACTIVE ENERGY **37**
REFERENCES **47**

Report Documentation Page

Form Approved
OMB No. 0704-0188

Public reporting burden for the collection of information is estimated to average 1 hour per response, including the time for reviewing instructions, searching existing data sources, gathering and maintaining the data needed, and completing and reviewing the collection of information. Send comments regarding this burden estimate or any other aspect of this collection of information, including suggestions for reducing this burden, to Washington Headquarters Services, Directorate for Information Operations and Reports, 1215 Jefferson Davis Highway, Suite 1204, Arlington VA 22202-4302. Respondents should be aware that notwithstanding any other provision of law, no person shall be subject to a penalty for failing to comply with a collection of information if it does not display a currently valid OMB control number.

1. REPORT DATE	2. REPORT TYPE	3. DATES COVERED
SEP 2009	**N/A**	**-**

4. TITLE AND SUBTITLE
Electronically Excited States and Their Role in Affecting Thermodynamic and Transport Properties of Thermal Plasmas

5a. CONTRACT NUMBER
5b. GRANT NUMBER
5c. PROGRAM ELEMENT NUMBER

6. AUTHOR(S)

5d. PROJECT NUMBER
5e. TASK NUMBER
5f. WORK UNIT NUMBER

7. PERFORMING ORGANIZATION NAME(S) AND ADDRESS(ES)
Dept Chemistry University of Bari, via Orabona 4, 70125 Bari Italy CNR IMIP Bari, via Amendola 122/D, 70125 Bari

8. PERFORMING ORGANIZATION REPORT NUMBER

9. SPONSORING/MONITORING AGENCY NAME(S) AND ADDRESS(ES)

10. SPONSOR/MONITOR'S ACRONYM(S)
11. SPONSOR/MONITOR'S REPORT NUMBER(S)

12. DISTRIBUTION/AVAILABILITY STATEMENT
Approved for public release, distribution unlimited

13. SUPPLEMENTARY NOTES
See also ADA562449. RTO-EN-AVT-162, Non-Equilibrium Gas Dynamics - From Physical Models to Hypersonic Flights (Dynamique des gaz non- equilibres - Des modeles physiques jusqu'au vol hypersonique), The original document contains color images.

14. ABSTRACT
The contribution of internal degrees of freedom to thermal-plasma properties has been investigated in a wide range of temperature and pressure. Thermodynamic functions have been calculated modelling in different ways the electronic levels of atomic species (ground-state, Debye-Hückel and confined-atom approximations). Frozen and reactive specific heats are strongly affected by electronic excitation whereas compensation effects smooth its influence on the total specific heat, i.e. the sum of frozen and reactive contributions. High-order Chapman-Enskog method has been applied to evaluate transport coefficients. The inclusion of electronically excited states have a twofold impact, reflecting the changes on thermodynamic properties and on transport cross sections of excited species. Results for atomic hydrogen, nitrogen and air plasmas are considered in this lecture.

15. SUBJECT TERMS

16. SECURITY CLASSIFICATION OF:			17. LIMITATION OF ABSTRACT	18. NUMBER OF PAGES	19a. NAME OF RESPONSIBLE PERSON
a. REPORT	b. ABSTRACT	c. THIS PAGE			
unclassified	**unclassified**	**unclassified**	**SAR**	**52**	

INTRODUCTION

The role of electronic excitation in affecting the thermodynamic and transport properties of thermal plasmas is a subject of large interest which is however often overlooked by the scientific community. The reasons of this underestimation are essentially due

1. to the small differences reported by different authors when comparing thermodynamic properties obtained by using partition functions of atomic species obtained inserting only the ground state term with the corresponding values obtained by inserting in the partition function all electronic states compatible with a given cut-off criterion;
2. to the same situation occurring when comparing transport properties obtained by inserting in the relevant equations either transport cross sections equal to the ground state for all electronic states or transport cross sections depending on the principal quantum number, *n*.

These two points allow to bypass the problems associated with accurate determinations of electronic partition functions as well as the more difficult problem of calculating the transport cross sections of electronically excited states. Of course this approach is in contradiction when computing radiative energy fluxes due to the presence of a multitude of electronically excited states in the medium. Moreover statements 1 and 2 are a consequence of compensation effects between the different contributions of the thermodynamic and transport properties of thermal plasmas rather than to an insensitivity of the relevant properties on the electronic excitation of atomic species. These aspects which have been extensively studied by our group for both thermodynamic and transport properties of thermal plasmas will be reported in the present lecture.

The paper is basically divided in two parts, the first one dedicated to clarify the role of electronic excitation on the thermodynamic properties of thermal plasmas; the second part treats the influence of electronically excited states on the transport properties of thermal plasmas.

For the thermodynamic properties we in particular discuss H_2 and N_2 plasmas. In the first case we limit our study to the partially ionized regime i.e. we suppose that our plasma is composed by H(n), H^+ and electrons and we report the dependence of the specific heats and isentropic coefficient γ (*frozen*, *reactive* and *total*) on the electronic contribution. The large differences observed in this plasma by comparing ground state and Debye-Hückel results are due to electronically excited states with principal quantum number $n>1$. An other interesting aspect studied in this case is the dependence of thermodynamic properties on the different energy levels inserted in the partition function of atomic hydrogen i.e. energy levels obtained by introducing in the Schrödinger equation the Coulomb potential or the Debye-Hückel potential. Large differences are observed at high pressure.

The nitrogen plasma case is indeed interesting because the partition function of atomic species (neutral, ionized) inserts both *low-lying* ($n=2$) and *high-lying* ($n>2$) electronically excited states. As an example the nitrogen atom presents two low-lying excited states (^2D, ^2P) and a multitude of high-lying electronically excited states mainly coming from the interaction of the optical electron (3s, 3p, 3d, 4s, 4p, 4d, 4f ...) and the nitrogen core (^3P). The low-lying excited states are able to affect the thermodynamic properties of nitrogen plasmas also in the dissociation regime, while the high-lying excited states are important for the different ionization regimes.

Different case studies are reported to emphasize the role of electronically excited states on the transport properties of thermal plasmas. We start again with the hydrogen atomic plasma. In this case we report the dependence of transport coefficients (*thermal conductivity*, *electrical conductivity* and *viscosity*) on the cut-off criterion (Debye-Hückel, confined-atom approximation, ground-state method) used for calculating the electronic partition function and therefore the concentrations of the relevant species entering in the transport equations. In a second step we study these effects by using a state-to-state approach i.e. by

considering each electronically excited state as a new species with its own transport cross section. In the hydrogen case the dependence of transport cross sections (diffusion and viscosity-type) of atomic hydrogen in the *n*-th principal quantum number with the other partners of the mixture (H(*n*), H^+ and electrons) is known. Interesting results are obtained including also the explanation of compensation effects arising in the calculation of transport coefficients by using the rigorous Chapman-Enskog method.

The extension of these ideas to air plasmas is discussed. At the moment the knowledge of transport cross sections for low-lying electronically excited states of oxygen and nitrogen atomic species (neutral and ionized) is well developed while the transport cross sections of high-lying excited atomic nitrogen and oxygen atoms is limited to the diffusion transport cross sections of excited atoms through ionized species. The present state of art of transport cross sections therefore allows us to study the influence of low-lying excited states on the internal thermal conductivity and of the viscosity of atmospheric air plasmas in the temperature range 5,000-12,000 K when high-lying excited states do not contribute to the transport coefficients. The role of high-lying excited states in affecting the transport coefficients can be inferred by scaling the transport cross sections of atomic oxygen and nitrogen electronically excited states with the corresponding hydrogen ones.

PART I : THERMODYNAMIC PROPERTIES

Thermodynamic properties of high pressure-high temperature plasmas are a research field of continuous interest due to their importance in different technological applications. Several research groups are presenting new results for different systems including plasmas [1,2] for aerospace applications, plasma mixtures generated in the chamber of inertial fusion energy reactors from the molten salts Flibe and Flinabe [3] salts and different gas mixtures for thermal plasma processing [4-5]. At the same time, high-temperature-high-pressure plasmas are important for astrophysics, e.g. for helioseismology [6]. The method of calculation in general starts with the determination of electronic partition functions and continues with the definition of the different thermodynamic properties of an ideal multi-component mixture with Debye-Hückel corrections. These corrections induce an iterative procedure due to interdependence of partition function and electron densities. Apparently the theory is well established even though many problems still exist. We refer in particular to the non-uniqueness equilibrium criteria [6-11] for multi-temperature plasmas as well as for the application of different mechanical statistical approaches [12-14] for the calculation of thermodynamic properties of very high pressure strongly coupled plasmas. Interesting in this context is the REMC (*Reaction Ensemble Monte Carlo*) [15] method i.e. a molecular level simulation method for calculating equilibrium compositions and thermodynamic properties of plasmas including Coulomb forces, ionization potential lowering and short range interactions.

Coming back to the multi-component ideal mixtures recent interest has been devoted to the role of electronic excitation in affecting the thermodynamic properties of an hydrogen plasma [16-20] under local thermodynamic equilibrium (LTE) conditions. The strong dependence of these quantities on the cut-off criterion used in calculating the atomic partition function has been observed [16-18]. In particular, use of Fermi's criterion, which excludes from the partition function levels with Bohr's radius exceeding the inter-particle distance, increases the importance of electronically excited states as compared with the results obtained by considering Griem cut-off, based on the Debye-Hückel theory [21,22]. This result is the consequence of the minor number of excited states considered in the calculation of the partition function and of its derivatives as well in the lowering of the ionization potential in the Saha equation. This last effect accelerates the ionization reaction thus decreasing the number density of H atoms, which, in the case of atomic hydrogen plasmas (H, H^+, e), is the only species possessing electronic energy. Use of Griem criterion decreases the importance of electronically excited states in affecting the thermodynamic properties of thermal plasmas also because some compensation effects arise in the self-consistent calculation. However, Griem cut-off criterion, as usually used, suffers of an important limitation. In fact, while the cut-off is determined self-consistently with the electron density, the energy levels considered in

the partition function are those derived from the Schrödinger equation inserting in it the Coulomb potential for electron-proton interaction. This is a strong limitation specially at high electron density when the Debye-Hückel potential predicts large variation in the H level energies [23] as compared with the Coulomb levels.

1.1 Hydrogen plasmas

We study the influence of the selection of energy levels (Coulomb versus Debye-Hückel potential) in affecting the properties of single species (partition function an specific heat) as well as typical mixture thermodynamic quantities. In particular, frozen, reactive and total specific heat of the LTE atomic hydrogen plasma mixture has been reported as a function of temperature in a wide range of pressure. To complete this study we consider also the dependence of the isentropic coefficient $\gamma=c_p/c_v$ on the electronic excitation, a quantity which plays an important role on the dynamical expansion of plasmas [6,24].

1.1.1 Method of calculation

Starting from a mole of atomic hydrogen and introducing the ionization degree α we can assume that the H, H^+, e moles are respectively 1-α, α, α.

For any species the translational molar enthalpy is given by $5/2RT$ and, being D the dissociation energy of H_2 and I the ionization energy of H atoms, D/2 and D/2+ I_H are respectively the chemical enthalpy of atomic hydrogen, and of protons, and denoting by E_H the electronic energy of atomic hydrogen, the total enthalpy (in J) of the plasma is given by

$$\begin{aligned} H &= \tfrac{5}{2}(1-\alpha)RT+\tfrac{5}{2}\alpha RT+\tfrac{5}{2}\alpha RT+(1-\alpha)(\tfrac{D}{2}+E_H)+\alpha(\tfrac{D}{2}+I_H)= \\ &= \tfrac{5}{2}(1+\alpha)RT+(1-\alpha)E_H+\tfrac{D}{2}+\alpha I_H \end{aligned} \tag{1.1}$$

Note that in this equation the lowering of the ionization potential has been neglected, while in the full calculation has been taken into account.

The frozen specific heat of the LTE atomic hydrogen plasma (H, H^+, e) is given by

$$c_{pf}=\left(\frac{\partial H}{\partial T}\right)_{p,\alpha}=(1+\alpha)\tfrac{5}{2}R+(1-\alpha)c_{vH} \tag{1.2}$$

where c_{vH} is the internal specific heat of atomic hydrogen which depends on the first and second logarithmic derivatives of the partition function i.e.

$$c_{vH}=k\left[\frac{d\ln f_H}{d\ln T}+\frac{d^2\ln f_H}{d^2\ln T}\right]=\frac{dE_H}{dT} \tag{1.3}$$

where f_H is the electronic partition function of atomic hydrogen.

The first term in Eq. (1) is the translational contribution to the frozen specific heat and the second term is the internal contribution which is the product of the internal specific heat of atomic hydrogen and its concentration. To calculate the ionization degree, we must solve the Saha's equation written in the form

$$k_p=\frac{\alpha^2}{(1-\alpha^2)}p=\frac{(2\pi m_e kT)^{5/2}}{h^3}\frac{2}{f_H}\exp-(I_H-\Delta I)/kT \tag{1.4}$$

where I is the ionization potential of the atomic hydrogen corrected for the lowering of the ionization potential ΔI. In turn ΔI depends, in the Griem approach, on the number density of the ionized species (electrons and protons). Therefore, an iterative procedure must be used for the calculation of ΔI and of the partition function written as

$$f_H = \sum_{n,\ell}^{n_{max},\ell_{max}} g_{n,\ell} \exp(-E_{n,\ell}/kT) \tag{1.5}$$

where n_{max}, ℓ_{max} are the quantum numbers of the last level to be inserted in the electronic partition function. According to Griem approach, this level is determined by the following inequality

$$E_{n_{max},\ell_{max}} \le I_H - \Delta I \tag{1.6}$$

Partition functions and their derivatives depend on the energy level values. We use two types of energy levels: the unperturbed energy levels obtained from the Coulomb potential $\varphi = -e^2/r$ and those obtained by considering the Debye-Hückel potential $\varphi = -(e^2/r)\exp(-r/\lambda)$ (λ is the *Debye length*) in the Schrödinger equation. For the Coulomb potential, we obtain the well known energy levels and statistical weights

$$\begin{aligned} E_n &= I_H\left(1-\frac{1}{n^2}\right) \\ g_n &= 2n^2 \end{aligned} \tag{1.7}$$

depending only on the principal quantum number n (I_H is the ionization potential of atomic hydrogen).

The Debye-Hückel levels have been obtained from the numerical solution of the Schrödinger equation inserting in it the screened Coulomb potential. A complete set of energy levels up to n=9 has been obtained by Roussel and O'Connell [23] and tabulated as a function of the Debye length λ for the different (n,ℓ) levels. The partition function in this case must be calculated allowing the (n,ℓ) structure with the appropriate statistical weights.

Let us consider now the total specific heat of the plasma mixture i.e. the derivative of the total enthalpy with respect to temperature at constant pressure. This quantity has been calculated in the present work by numerical derivative of the total enthalpy including also the lowering of the ionization potential. A simplified expression can be obtained from Eq. (1.1) getting

$$\begin{aligned} c_p = c_{pf} + c_{pr} = \left(\frac{\partial H}{\partial T}\right)_p &= (1+\alpha)\tfrac{5}{2}R + (1-\alpha)c_{vH} \\ &+ \frac{1}{RT^2}\frac{\alpha(1-\alpha^2)}{2}\left(I_H + \frac{5RT}{2} - E_H\right)\left(I_H + \frac{5RT}{2} - E_H\right) \end{aligned} \tag{1.8}$$

which can be thought as the sum of frozen and reactive contributions i.e.

$$\begin{aligned} c_{pf} &= \left(\frac{\partial H}{\partial T}\right)_{p,\alpha} = (1+\alpha)\tfrac{5}{2}R + (1-\alpha)c_{vH} \\ c_{pr} &= \left(\frac{\partial H}{\partial \alpha}\right)_{p,\alpha}\left(\frac{\partial \alpha}{\partial T}\right)_p = \frac{1}{RT^2}\frac{\alpha(1-\alpha^2)}{2}\left(I_H + \frac{5RT}{2} - E_H\right)\left(I_H + \frac{5RT}{2} - E_H\right) \end{aligned} \tag{1.9}$$

Note that in this equation we are using the Van't Hoff treatment of the equilibrium constant written in the classical form

$$k_p = \frac{\alpha^2}{(1-\alpha^2)} p = \frac{\alpha^2 RT}{(1-\alpha)V} = \exp(\Delta S/R)\exp(-\Delta H/RT) \tag{1.10}$$

for obtaining $(\partial\alpha/\partial T)_p$ and considering ΔH and ΔS independent of temperature. It should be noted that the form $\alpha^2 RT/(1-\alpha)V$ is obtained by considering the equation of state

$$pV = (1+\alpha)RT \tag{1.11}$$

All the quantities are expressed in Joule/K. In the present case, because the total mass is 1 g, same values are for J/K/g.

To get the isentropic coefficient $\gamma=c_p/c_v$ we have solved the thermodynamics of the plasma mixture alternatively imposing constant pressure and volume constraints. In both cases the total specific heats have been calculated by numerical derivation of the total enthalpy and total energy with respect to the temperature by imposing the appropriate constraints.

To better understand the numerical results, we report an analytical formula of the isentropic coefficient based on the classical thermodynamics. We must first write the total energy as

$$\begin{aligned} E &= \tfrac{3}{2}(1-\alpha)RT + \tfrac{3}{2}\alpha RT + \tfrac{3}{2}\alpha RT + (1-\alpha)(\tfrac{D}{2} + E_H) + \alpha(\tfrac{D}{2} + I_H) = \\ &= \tfrac{3}{2}(1+\alpha)RT + (1-\alpha)E_H + \tfrac{D}{2} + \alpha I_H \end{aligned} \tag{1.12}$$

Then we can calculate

$$c_{vf} = \left(\frac{\partial E}{\partial T}\right)_{V,\alpha} = \tfrac{3}{2}(1+\alpha)R + (1-\alpha)c_{vH} \tag{1.13}$$

$$c_{vr} = \left(\frac{\partial E}{\partial \alpha}\right)_{V,\alpha}\left(\frac{\partial \alpha}{\partial T}\right)_V = \frac{1}{RT^2}\frac{\alpha(1-\alpha)}{(2-\alpha)}\left(I_H + \frac{3RT}{2} - E_H\right)\left(I_H + \frac{3RT}{2} - E_H\right) \tag{1.14}$$

$$c_v = c_{vf} + c_{vr} \tag{1.15}$$

To get $(\partial\alpha/\partial T)_V$ one should consider the classical equilibrium constant (i.e. Eq. (1.10)) as a function of V.

Therefore we obtain for the isentropic coefficient of atomic hydrogen plasma the following equation

$$\gamma = \frac{c_p}{c_v} = \frac{\left[\frac{1}{RT^2}\frac{\alpha(1-\alpha^2)}{2}\left(I_H + \frac{5RT}{2} - E_H\right)\left(I_H + \frac{5RT}{2} - E_H\right) + (1+\alpha)\tfrac{5}{2}R + (1-\alpha)c_{vH}\right]}{\left[\frac{1}{RT^2}\frac{\alpha(1-\alpha)}{(2-\alpha)}\left(I_H + \frac{3RT}{2} - E_H\right)\left(I_H + \frac{3RT}{2} - E_H\right) + (1+\alpha)\tfrac{3}{2}R + (1-\alpha)c_{vH}\right]} \tag{1.16}$$

This equation assumes simplified forms for the following extreme cases

- for an atomic neutral gas i.e. $\alpha=0$

$$\gamma = \frac{c_p}{c_v} = \frac{\left[\frac{5}{2}R + c_{vH}\right]}{\left[\frac{3}{2}R + c_{vH}\right]} \tag{1.17}$$

yielding a value $\gamma = \frac{c_p}{c_v} = \frac{5}{3} = 1.666$ when electronic excitation is not considered (i.e when $c_{vH} = 0$).

- for a fully ionized atomic hydrogen plasma (α=1) again we obtain

$$\gamma = \frac{c_p}{c_v} = \frac{5}{3} = 1.666 \tag{1.18}$$

- for a partially ionized gas in the absence of electronic excitation of hydrogen atoms (i.e. when $E_{vH} = 0$ and $c_{vH} = 0$) we obtain

$$\gamma = \frac{c_p}{c_v} = \frac{\left[\frac{1}{RT^2}\frac{\alpha(1-\alpha^2)}{2}\left(I_H + \frac{5RT}{2}\right)^2 + (1+\alpha)\frac{5}{2}R\right]}{\left[\frac{1}{RT^2}\frac{\alpha(1-\alpha)}{(2-\alpha)}\left(I_H + \frac{3RT}{2}\right)^2 + (1+\alpha)\frac{3}{2}R\right]} \tag{1.19}$$

In the last equation are well evident in both numerator and denominator the reactive and translational contributions to the isentropic coefficient.

Finally the frozen isentropic coefficient for the atomic plasma assumes the form

$$\gamma_{frozen} = \left(\frac{c_p}{c_v}\right)_{frozen} = \frac{\left[(1+\alpha)\frac{5}{2}R + (1-\alpha)c_{pA}^{el}\right]}{\left[(1+\alpha)\frac{3}{2}R + (1-\alpha)c_{pA}^{el}\right]} \tag{1.20}$$

It should be noted that the frozen isentropic coefficient keeps a constant value of 5/3 as a function of temperature independently of the ionization degree when we neglect the electronic excitation i.e.

$$\gamma_{frozen} = \left(\frac{c_p}{c_v}\right)_{frozen} = \frac{\left[(1+\alpha)\frac{5}{2}\right]}{\left[(1+\alpha)\frac{3}{2}\right]} = \frac{5}{3} \tag{1.21}$$

which is recognized as the value for inert mono-atomic gases with only translational degrees of freedom.

1.1.2 Thermodynamic properties

In this section, we compare results obtained by considering

- (*curve a*) energy levels from the Debye-Hückel potential [23]
- (*curve b*) energy levels from the Coulomb potential
- (*curve c*) only hydrogen ground state (f_H= 2, $c_{p,int}$(H)=0).

For *curves a* and *b* the number of levels is truncated by using the Griem cut-off, calculated self-consistently with the plasma composition.

All the results have been calculated by using a self-consistent cut-off. From a qualitative point of view, it can be expected that the use of Debye-Hückel energy levels should increase the electronic partition function and its derivatives as compared with the corresponding results obtained by using energy levels

from the Coulomb potential. The action of the Debye-Hückel potential in fact is to decrease the energy of the levels as the Debye length decreases and to increase the Boltzmann factors as well as the number of levels included in the electronic partition function calculation, this last effect being predominant. The increase in the electronic partition function generates an increase of the atomic-hydrogen molar fractions and, in turn, increases the importance of electronic excitation on the thermodynamic properties of the plasma.

Figure 1.1 shows the self-consistent partition functions calculated with the two sets of levels as a function of temperature for different pressures. We can see, as expected, that the Debye-Hückel levels increase the partition function as compared with the corresponding values obtained by Coulomb potential. The effects are appreciable for p>10 atm.

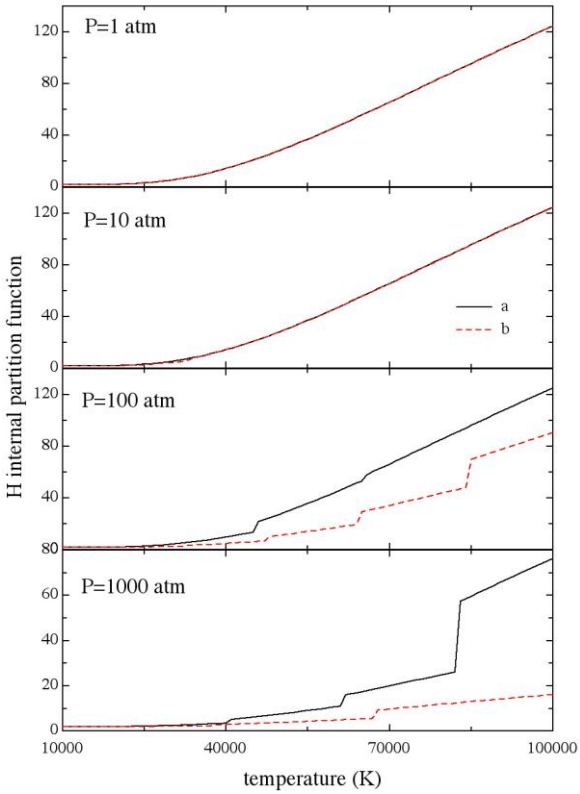

Fig. 1.1. Electronic partition function of atomic hydrogen as a function of temperature at different pressures (*curves a-b* as explained in the text).

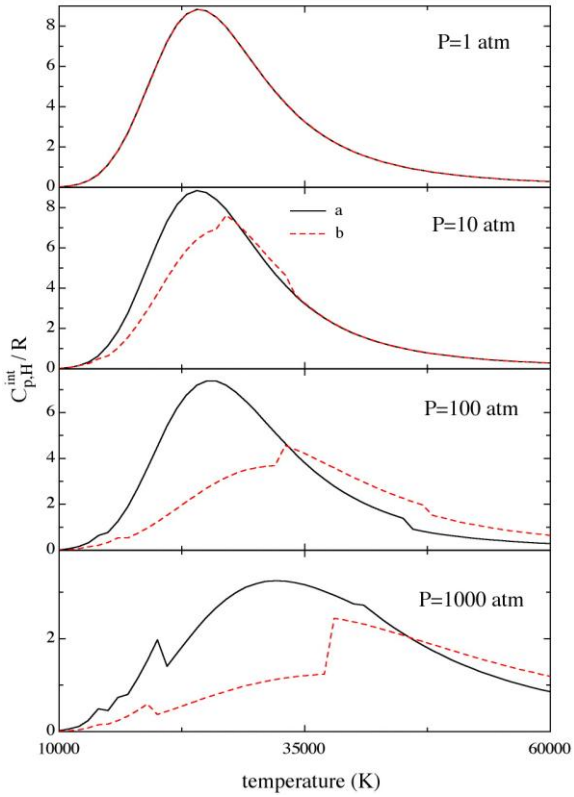

Fig. 1.2. Internal specific heat of atomic hydrogen as a function of temperature at different pressures (*curves a-b* as explained in the text).

Figure 1.2 shows the trend of the internal specific heat of atomic hydrogen normalized to R. In this case some differences appear also at 10 atm. Note that the specific heat calculated with the Debye-Hückel levels overcomes the corresponding values from the Coulomb potential in a large temperature range, reversing the trend from a given temperature depending on pressure. This behavior is due to the first and second derivatives of the partition function. Note also that the discontinuities present in the partition function and in the specific heat are due to the abrupt change of the number of energy levels entering in the different quantities.

Figure 1.3 shows the frozen specific heat of the mixture calculated with the two series of levels. The largest differences occur at p=100 atm. as a result of the combined effect of the specific heat of atomic hydrogen and of the molar fraction of the same species. Note that in any case the frozen specific heat calculated from the Debye-Hückel levels overcomes the corresponding quantity calculated from Coulomb levels in all the considered temperature range. The maximum deviation can reach a value of 40%. This result is the consequence of the internal contribution of atomic hydrogen on the frozen specific heat of the mixture (see Eq. (1.1)). In Figure 1.3 we have also reported the frozen specific heat calculated by completely disregarding the internal electronic contribution of atomic hydrogen either in the equilibrium composition or in the thermodynamic quantities (*ground-state model*). Comparison of these values with those reported in *curves (a)* and *(b)* gives an idea of the importance of electronic excitation on the frozen specific heat of the mixture.

Let us now consider the reactive contribution to the total specific heat. Inspection of Eq. (1.8) shows that the internal energy has a negative effect on this contribution, as illustrated in Fig. 1.4. The *curves (c)* correspond to the ground-state model which is characterized by completely neglecting of the electronically excited states in the partition function and its derivatives. Ground-state results overestimate the reactive contribution up to 15%.

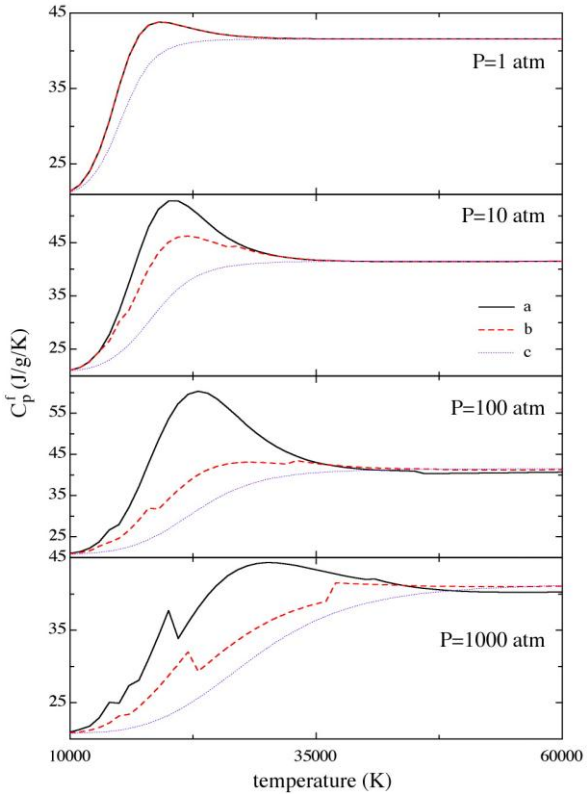

Fig. 1.3. Frozen contribution to constant-pressure specific heat of the plasma mixture (H, H^+, e) at as a function of temperature at different pressures (*curves a-c* as explained in the text).

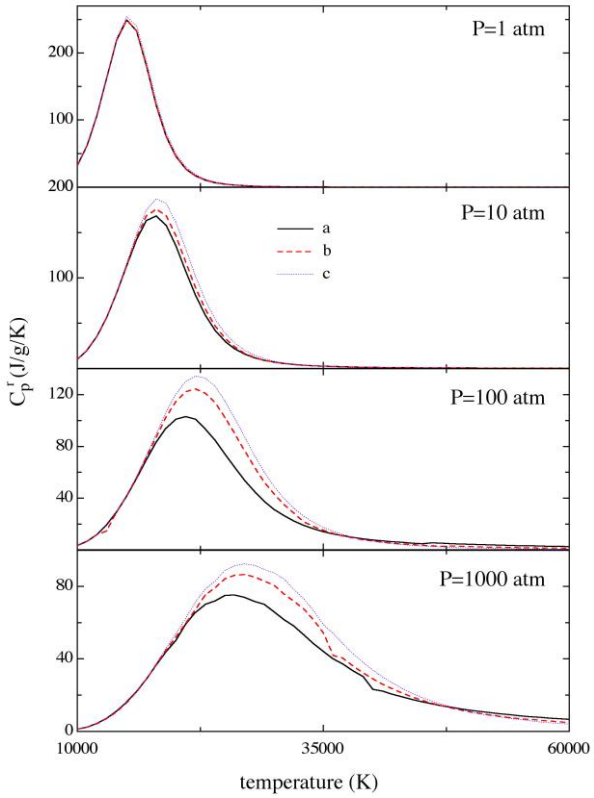

Fig. 1.4. Reactive contribution to constant-pressure specific heat of the plasma mixture (H, H^+, e) at as a function of temperature at different pressures (*curves a-c* as explained in the text)

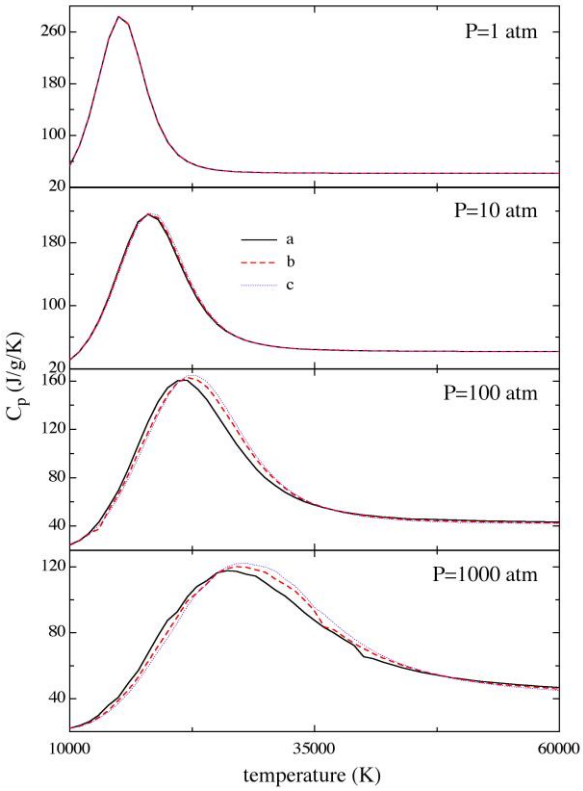

Fig. 1.5. Total constant-pressure specific heat of the plasma mixture (H, H^+, e) as a function of temperature at different pressures (*curves a-c* as explained in the text).

A sort of compensation appears in the total specific heat thus decreasing the role of electronically excited states in affecting this quantity (see Fig. 1.5). We see that in this case the differences, even still existing, strongly decrease, the maximum deviation being of the order of few percents. This point , already reported by one of the present authors many years ago [24], should not confuse the reader on the importance of electronically excited states in affecting the thermodynamic properties of thermal plasmas.

1.1.3 Isentropic coefficients

We discuss now the isentropic coefficients following the same lines previously reported i.e. we compare the results for *cases a*, *b* and *c* previously defined. In particular Figure 1.6 reports the frozen isentropic coefficients as a function of temperature for different pressures, while Figure 1.7 reports the corresponding total isentropic coefficients.

Inspection of Figure 1.6 shows the strong dependence of the frozen isentropic coefficient on the electronic excitation. This coefficient in the absence of electronic excitation keeps a constant value of 1.666 as already pointed out (see Eq. (1.21)). The strong minima present in Fig. 1.6 are the result of the electronic contribution to atomic hydrogen specific heat; the value of the minimum strongly depends on the pressure, the maximum effect occurring at 100 atm. In this case the isentropic coefficient for *case (a)* i.e. for the self-consistent Debye-Hückel treatment for both cut-off criterion and energy levels presents a value of 1.25 to be compared with the value of 1.666 *(case c)* occurring in the absence of electronic excitation. It should be also noted the importance of the self-consistent Debye-Hückel energy levels in affecting the isentropic coefficient when comparing the minimum value of case a (i.e. 1.25) with the corresponding minimum obtained with the Coulomb energy levels (i.e. 1.45).

The contribution of electronic term tends to be masked in the total isentropic coefficient which includes reactive, translational and electronic contributions as can be appreciated from Fig. 1.7. In fact in this case calculated values for the *cases a-c* differ by not more than 5% as a result of some compensation in the different terms of Eq. (1.16).

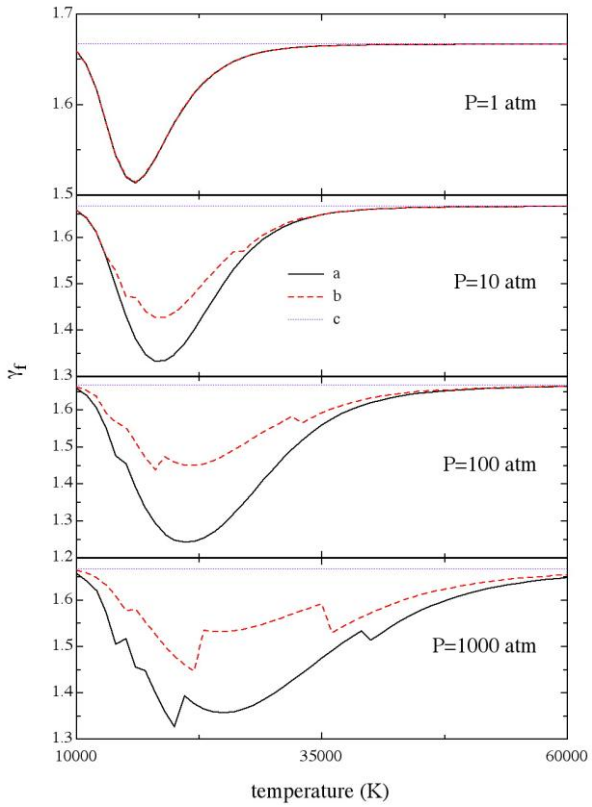

Fig. 1.6. Frozen isentropic coefficient of the plasma mixture (H, H^+, e) as a function of temperature at different pressures (*curves a-c* as explained in the text).

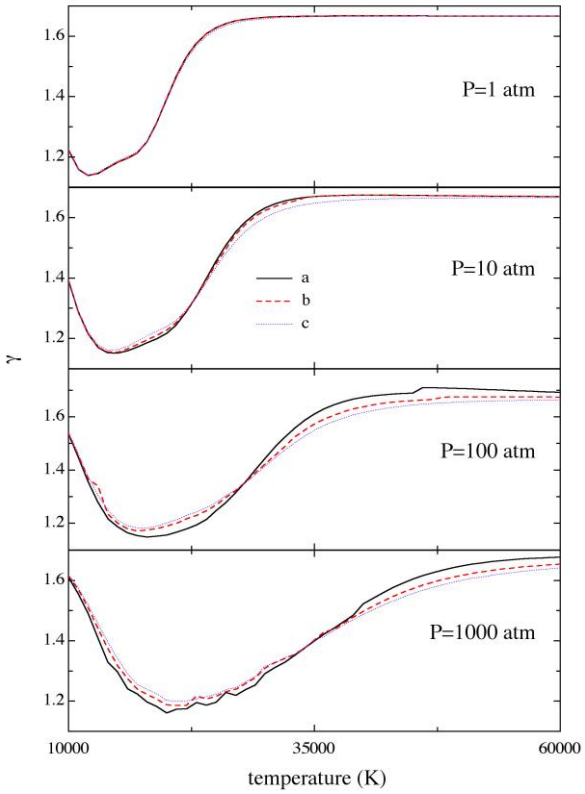

Fig. 1.7. Total isentropic coefficient of the plasma mixture (H, H^+, e) as a function of temperature at different pressures (*curves a-b* as explained in the text).

1.2 Nitrogen plasmas

1.2.1 Thermodynamic properties

Let us consider as a second example a nitrogen plasma in the conditions similar to those examined for the atomic hydrogen plasma. We consider now the following species N_2, N, N^+, N^{+2}, N^{+3}, N^{+4}, e linked by the equilibria

$$N_2 = 2N$$
$$N = N^+ + e$$
$$N^+ = N^{+2} + e$$
$$N^{+2} = N^{+3} + e$$
$$N^{+3} = N^{+4} + e$$

The calculations we report have been calculated by a self-consistent approach described in Ref. [1]. Briefly the electronic partition functions of atomic species (neutral, ionized) are calculated by inserting all levels (tabulated and unknown) the energy of which is less than the lowering of the ionization potential i.e.

$$f_{ej} = \sum_{0}^{E_{njmax}} g_{nj} \exp(-E_{nj}/kT) \qquad (1.22)$$

where E_{nj} and g_{nj} represent in the order the energy and the statistical weight of the n-th level of the j-th species. The sum includes all levels up to a maximum value given by

$$E_{njmax} = I_j - \Delta I_{j,j+1} \tag{1.23}$$

In turn the lowering of the ionization potential $\Delta I_{j,j+1}$ is given according to the Debye-Hückel (DH) theory by

$$\Delta I_{j,j+1} = \frac{e^3}{\zeta^{3/2}} \sqrt{\frac{\pi}{kT}} \left(\sum_{i=1}^{n} z_i^2 n_i\right)^{1/2} 2(z_j + 1) \tag{1.24}$$

Debye-Hückel corrections are also used to correct the thermodynamic properties of plasmas. Relevant results are then compared with the corresponding ones obtained by the *ground-state* method (GS) i.e.

$$f_{ej} = g_{0j} \tag{1.25}$$

Let us consider first the properties of single species.

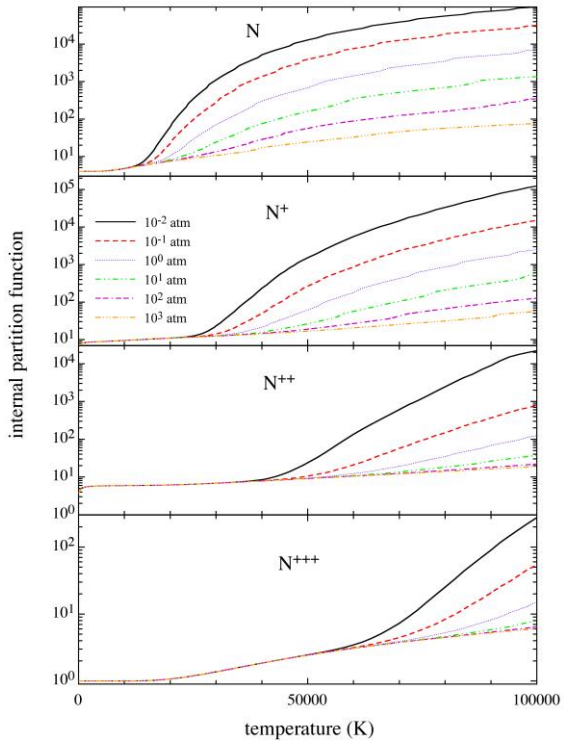

Fig. 1.8. Electronic partition function of N, N^+, N^{+2}, N^{+3} species as a function of temperature at different pressures.

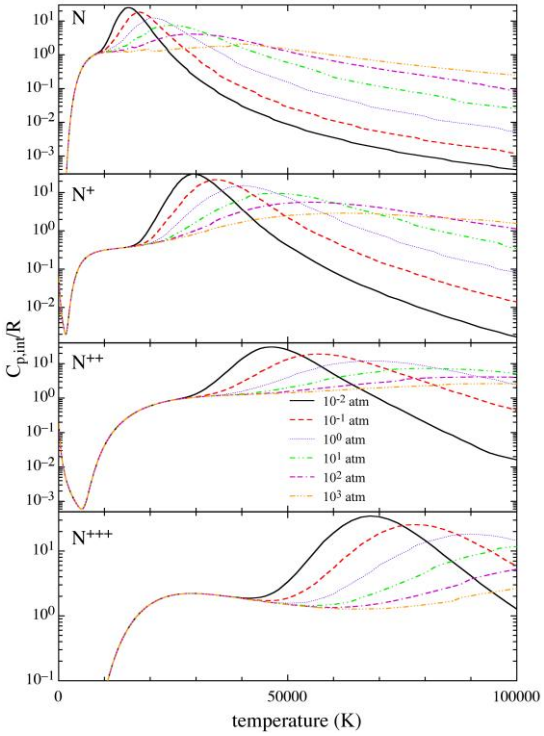

Fig. 1.9. Internal specific heat of of N, N^+, N^{+2}, N^{+3} species as a function of temperature at different pressures.

Figure 1.8 compares the electronic partition function of the nitrogen species calculated by applying DH and GS methods as a function of temperature for different pressures. To understand these figures we report in the following the statistical weights of the ground states of the different species. We obtain

$$\begin{aligned} &N(^4S_{1.5});\ N^+(^3P_{2,1,0});\ N^{+2}(^2P_{1.5,0.5});\ N^{+3}(^1S_0);\ N^{+4}(^2S_{0.5}) \\ &g(N(^4S_{1.5}))=4;\ g(N^+(^3P_{2,1,0}))=9;\ g(N^{+2}(^2P_{1.5,0.5}))=6;\ g(N^{+3}(^1S_0))=1;\ g(N^{+4}(^2S_{0.5}))=2 \end{aligned} \tag{1.26}$$

These values persist for all temperature and pressure ranges for the different species in the GS approximation. The insertion of electronic states is such to enormously increase the electronic partition functions of nitrogen species. It should be also noted the role played by the so called *low-lying* (valence) levels in affecting the partition function in the relatively low temperature regime followed by the enormous role played by *high-lying* excited states (i.e. states with principal quantum numbers n>2). This last effect is strongly dependent on pressure.

It should be noted that only the $N^{+3}(^1S_0)$ does not possess low-lying excited states so its partition function starts increasing from its 1 value up to the insertion on the electronic partition function of high-lying electronically excited states. On the other hand the species N, N^+, N^{+2} possess low-lying excited states so that their partition functions are different from their ground state statistical weights at temperature lower than 10,000 K.

The temperature dependence of partition function is reflected on the first and second logarithmic derivatives and on the quantities depending on them. As an example we report in Fig. 1.9 the electronic specific heats of the species N, N^+, N^{+2}, N^{+3} as a function of temperature for different pressures calculated according to the DH theory. Keeping in mind that the corresponding values from GS method is zero, we can understand the dramatic role of electronic excitation in affecting the specific heats of atomic species.

In this figure we can appreciate the role of low-lying and high-lying excited states in affecting the specific heat. It should be noted that the unusual behaviour of c_p for N^+, N^{+2} species at very low temperatures is due to energy splitting of the ground state levels.

Let us now examine the behaviour of the enthalpy variation of the different ionization processes. We select in particular

$$\begin{aligned} N &= N^+ + e \\ N^+ &= N^{+2} + e \\ N^{+2} &= N^{+3} + e \end{aligned}$$

We can write respectively

$$\begin{aligned} \Delta H_1 &= \tfrac{5}{2}kT + \varepsilon_1 - kTf'_{\text{int}\,N} + kTf'_{\text{int}\,N^+} \\ \Delta H_2 &= \tfrac{5}{2}kT + \varepsilon_2 - kTf'_{\text{int}\,N^+} + kTf'_{\text{int}\,N^{+2}} \\ \Delta H_3 &= \tfrac{5}{2}kT + \varepsilon_3 - kTf'_{\text{int}\,N^{+2}} + kTf'_{\text{int}\,N^{+3}} \end{aligned} \qquad (1.27)$$

where ε_1, ε_2 and ε_3 represent, in the order, the first, second and third ionization potentials of nitrogen corrected by the corresponding lowering and kTf'_{int} the corresponding internal energy of the relevant species (f'_{int} is the first logarithmic derivative of the partition function).

Values of ΔH for the ionization reactions calculated at different pressures according to DH and GS methods have been plotted as a function of temperature in Fig. 1.10. We can note strong differences between the linear increase of ΔH calculated according to the ground state method and the corresponding quantities calculated by using the Debye-Hückel theory. In this last case in fact ΔH goes through a minimum and can become larger than the ground state value. This is the consequence of taking into account the excitation energies of the species relevant to each reaction which occur in different temperature ranges. As an example, for the first ionization reaction, beyond the minimum of $\Delta H/T$ curves the electronic excitation of the ionized species $kTf'_{\text{int}\,N^+}$ begins to contribute to ΔH while the term $kTf'_{\text{int}\,N}$ is now decreasing with increasing temperature.

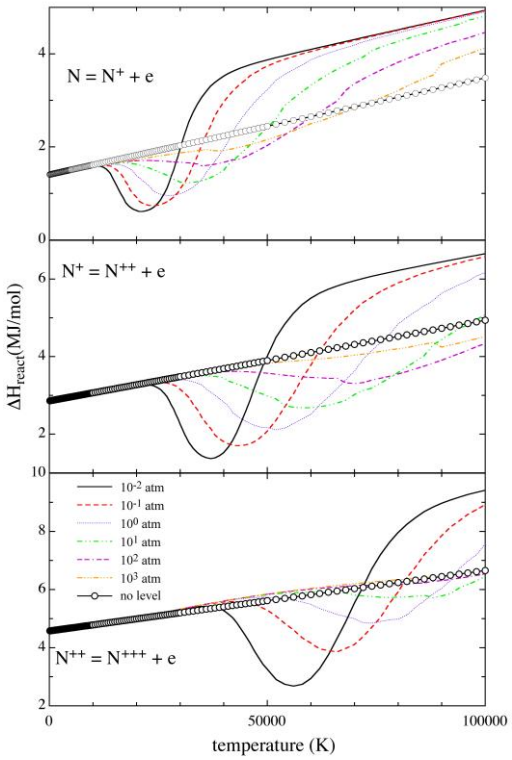

Fig. 1.10. Enthalpy of nitrogen ionization reactions as a function of temperature at different pressures.

Figures 1.11-1.13 report the specific heat (frozen, reactive, total) of nitrogen plasma as a function of temperature calculated according to the Debye-Hückel and the ground-state methods. The results can be rationalized on the basis of previous considerations on hydrogen plasmas, taking into account the different ionization processes in the nitrogen plasma. In particular the frozen specific heat is positively affected by the presence of electronically excited states for all ionization reactions. On the contrary the reactive specific heat for the first two ionization reactions is negatively affected by excited states as in the case of atomic hydrogen. The situation is much more complicated for the very high temperature regime (T>50,000 K) where the two sets of results (DH and GS approaches) considerably differ. Figure 1.14 reports the percentage difference in the specific heats calculated by using DH and GS methods. Again we see a compensation between frozen and reactive contributions in the total specific heat, this compensation tending to disappear for T>50,000 K. An interesting effect is also present in the first peak of both reactive and total specific heats. This peak is due to the dissociation reaction which is affected by the presence of electronically excited states in both atomic, N, and molecular, N_2, species. This effect strongly increases in going from p=1 atm to p=1000 atm.

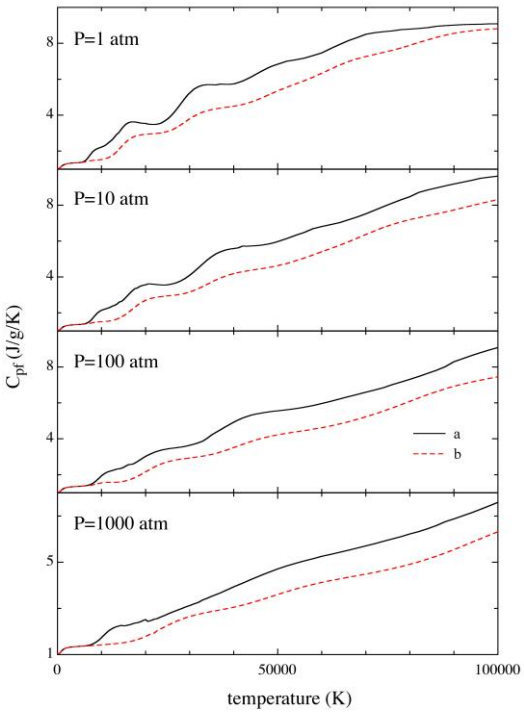

Fig. 1.11. Frozen contribution to constant-pressure specific heat of the nitrogen plasma at as a function of temperature at different pressures.

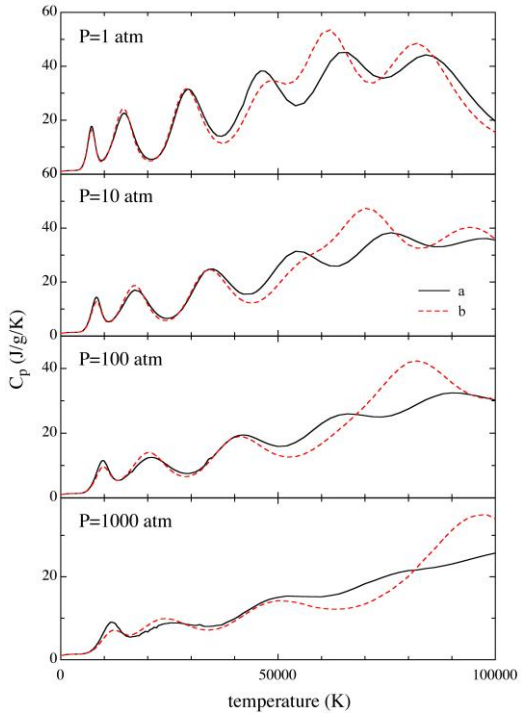

Fig. 1.13. Total constant-pressure specific heat of the nitrogen plasma as a function of temperature at different pressures.

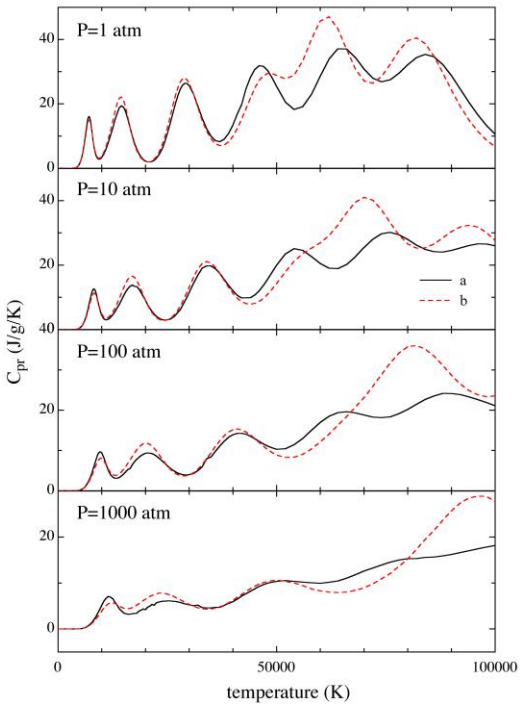

Fig. 1.12. Reactive contribution to constant-pressure specific heat of the nitrogen plasma at as a function of temperature at different pressures.

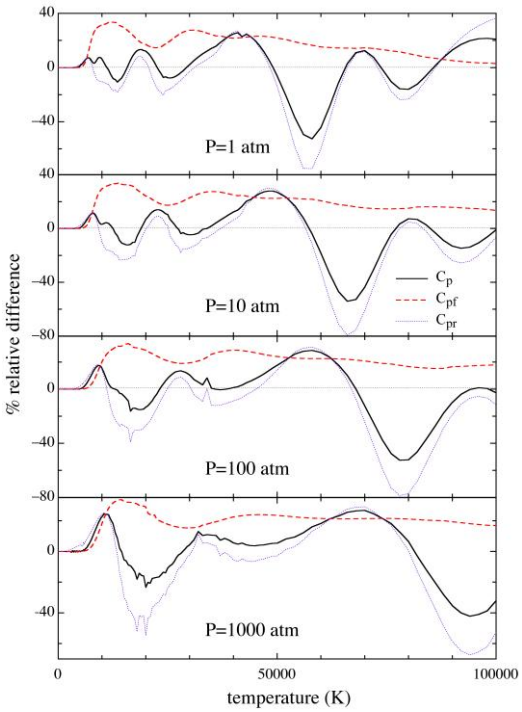

Fig. 1.14. Relative differences in the total specific heat and its components between *cases a* and *b* as a function of temperature at different pressures. 1.2.2 Isentropic coefficients

Figures 1.15 and 1.16 respectively report the frozen and total isentropic coefficients for nitrogen plasmas calculated with (*curves a*) and without (*curves b*) electronic excitation. The role of electronic excitation is well evident in both cases and can be rationalized extending the previous considerations for atomic hydrogen plasmas. In addition we can note for both frozen and total isentropic coefficients that at very low

temperature (100-3,000 K), i.e. when only molecular nitrogen is present, γ changes from the value of 1.4 (T≈100 K) to 1.3 (T≈3,000 K). The first value corresponds to the excitation of translational and rotational degrees of freedom of N_2, the second value to the excitation of vibrational, translational and rotational degrees of freedom.

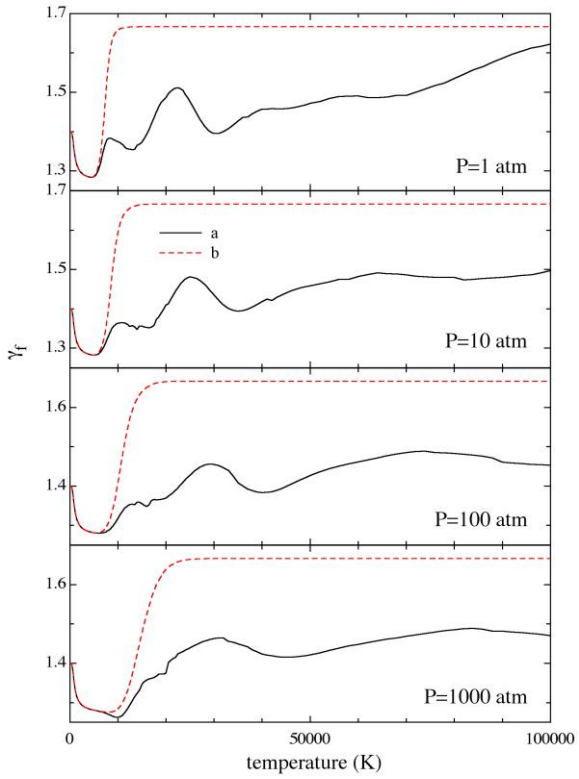

Fig. 1.15. Frozen isentropic coefficient of the nitrogen plasma as a function of temperature at different pressures.

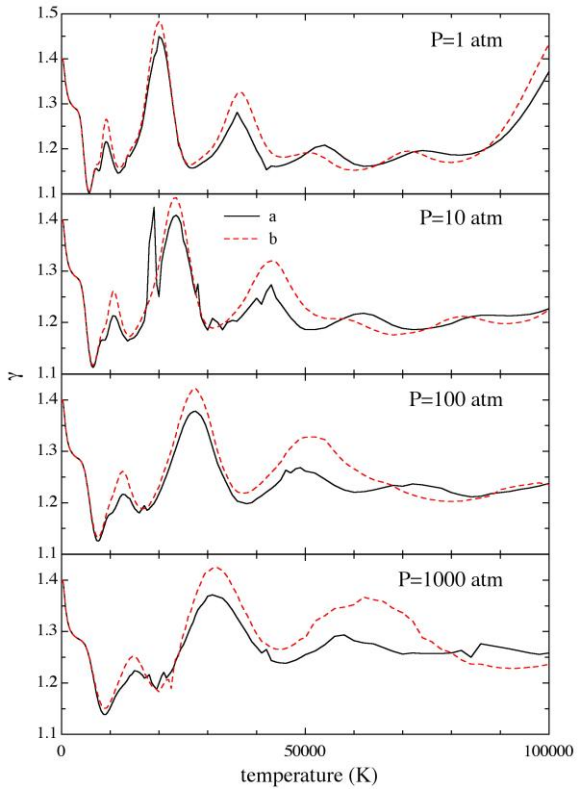

Fig. 1.16. Total isentropic coefficient of the nitrogen plasma as a function of temperature at different pressures.

PART II : TRANSPORT PROPERTIES

The role of electronically excited states (EES) in affecting the transport properties of thermal plasmas is a topic of renewed interest as attested by numerous contributions appearing in the literature [19,20,25-29]. Electronically excited states modify the composition and the thermodynamic (internal energy, specific heat) properties of the plasma, both quantities entering in the relevant transport equations. Moreover they present transport cross sections which dramatically increase as a function of the principal quantum number *n* determining unusual effects in the transport equations. Previous work presented by our group on atomic hydrogen plasma (H(*n*), H^+ and electrons) has shown these effects either in a parametric form [25,26] or by comparing the results obtained by the so called *ground-state method* (GS) with the corresponding ones obtained by the *confined-atom method* (CA) [19,20]. The first method (GS) completely disregards the presence of electronically excited states by imposing an electronic partition function of atomic hydrogen equal to 2 i.e. to the degeneracy of the ground state. As a consequence internal energy and specific heat of atomic hydrogen is zero in this approximation. The confined atom (CA) approximation inserts in the electronic partition function of atomic hydrogen all levels whose Bohr radius does not exceed the inter-particle distance. This method can be considered well representative for describing high pressure-high temperature plasmas. An other method very often used in truncating the electronic partition function is the Griem method [22], essentially based on the Debye-Hückel theory (DH) of electrolytes i.e. on the static screening Coulomb potential model. The three models (GS, CA, DH) have been extensively used to calculate the composition and the thermodynamic properties of atomic hydrogen plasmas to be inserted in the Chapman-Enskog formulation of the transport coefficients [30]. At the same time the effect of inserting actual transport cross sections, i.e. cross sections depending on the principal quantum number of electronically excited states, in the three thermodynamic models has been tested by comparing the results with the corresponding ones obtained by imposing the ground state cross section to all electronically excited states.

2.1 Hydrogen plasmas

2.1.1 Cut-off of the atomic partition function

In the first part of our lecture we have shown the strong dependence of partition function on the number of levels included in it. Although methods have been developed to correctly account for non-ideal effects in the thermodynamics of dense plasmas [31,32], these methods cannot be directly extended to a transport theory. Several simplified models are currently used in practice [33]:

- Ground state (GS) model. In this simplest case only the ground state is considered;
- Confined atom (CA) model. Those excited states whose size exceeds the inter-particle separation are excluded from the summation;
- Static screening Coulomb potential (DH) model. This model attempts to simulate the intra-atomic effects of the Debye-shielded Coulomb interactions.

The effect of the different criteria on the equilibrium composition of the plasma is shown in Fig. 2.1 for hydrogen plasma at different pressures. Reference results obtained from a sophisticated model [34] are reported for comparison indicating a satisfactory agreement specially with the CA model.

It is worth mentioning that the DH model, at variance from the other two, entails a pressure-dependent lowering of the ionization threshold. This has a deep influence on the equilibrium ionization degree, especially at large pressure where this effect becomes significant.

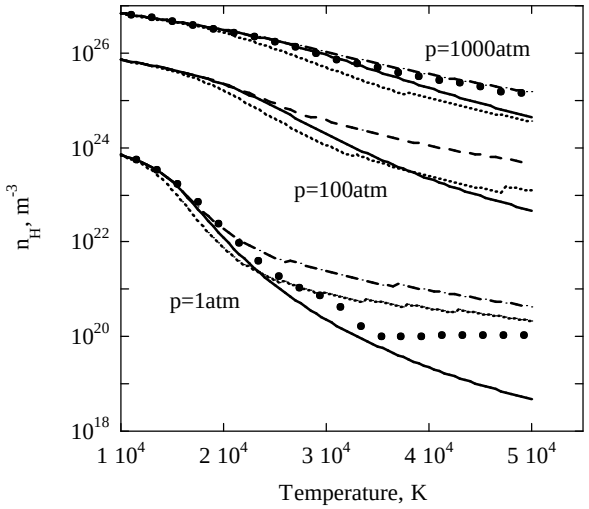

Figure 2.1. Hydrogen atom number density for equilibrium hydrogen plasma at different pressures as obtained by different cut-off models (solid line: GS; dashed line: CA; dotted line: DH; symbols: from Ref. [31]).

2.1.2 Collision integrals of electronically excited states

The calculation of the transport coefficients is straightforward once the collision integrals describing the interaction among different plasma constituents are specified. In order to properly account for the presence of EES, each electronic excited state of the hydrogen atom, H(*n*), *n* being the principal quantum number, is considered as a separate species. The collision integrals for the relevant interactions among H(*n*), H^+ and electrons are the same used in our previous works [25,26]. They present a strong dependence on the principal quantum number especially for collision integrals diffusion-type of H(*n*)-H^+ collisions. A sample of results is reported in Figs. 2.2a-b where we show the temperature dependence of the H(*n*)-H^+ collision integrals for selected values of the principal quantum number.

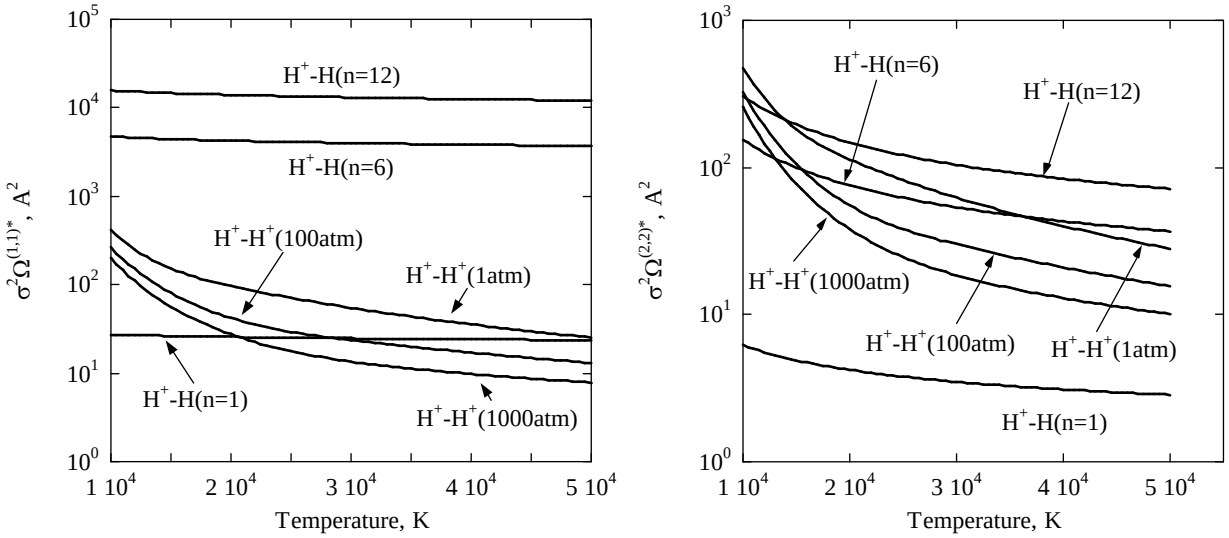

Figure 2.2. Temperature dependence of diffusion- and viscosity-type collision integrals for H(*n*)-H^+ interactions for selected values of the principal quantum number *n* and for the H^+-H^+ interaction at two pressures.

These are compared to the Coulomb collision integrals H^+-H^+ at three different pressures. We note that the latter depend on pressure through the Debye length which is a function of the electron concentration. The reported H(n)-H^+ collision integrals at high temperature are higher than the corresponding H^+-H^+ values.

2.1.3 Transport properties

Results are reported for the viscosity, thermal conductivity and electrical conductivity of equilibrium hydrogen plasma. These coefficients are obtained in the framework of the Chapman-Enskog method; the first non-vanishing approximation in terms of Sonine polynomials [19,20] has been used to estimate the heavy particle contributions and the second for the electron component [35].

2.1.3.1 Influence of composition and thermodynamic properties

The first effect of the different cutoff criteria is to produce differences in the equilibrium composition of the plasma. In order to show the extent of this influence, transport coefficients are calculated by using for EES the same cross sections as the ground state.

Figure 2.3 reports the comparison of the translational thermal conductivity of heavy particles for different plasma pressures as calculated under the three cutoff models. The thermal conductivity of atoms grows monotonously with temperature and is obviously independent of pressure. It is the large charge-exchange and Coulomb cross sections (see Figs. 2.2a-b) that make the conductivity decreasing as the proton concentration increases. When the plasma approaches the fully ionized limit, the coefficient grows again because the Coulomb cross sections decrease with temperature. The differences in the predictions of the three models are therefore explained by the differences in ionization degree. While at p=1 atm the differences are small, at higher pressures they can be very important. The DH model produces a higher ionization due to the insertion of the lowering of ionization potential and the predicted coefficient is smaller. The results of the GS model lie somewhat in between the other two: it follows the CA results at low temperature and then tend to the fully ionized limit at high temperature. The CA model instead, predicts a larger atom concentration at high temperature.

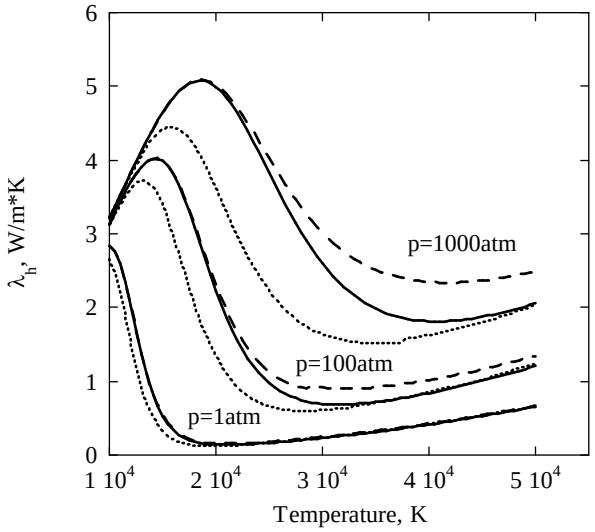

Figure 2.3. Translational thermal conductivity of heavy particles of equilibrium hydrogen plasma at different pressures. *Usual* values for the transport cross sections (solid line: GS; dashed line: CA; dotted line: DH).

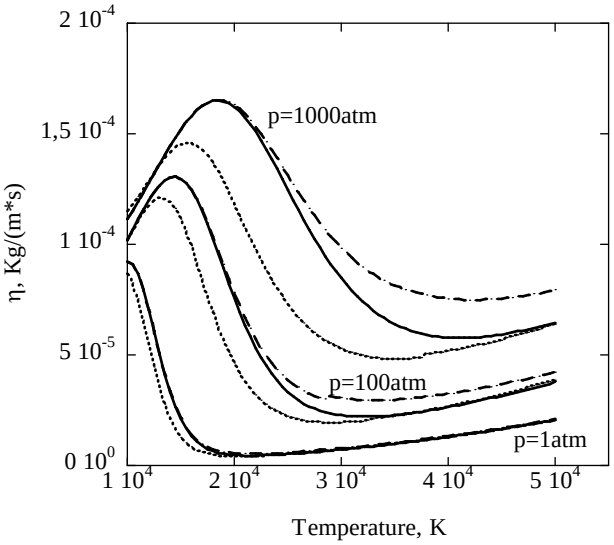

Figure 2.4. Viscosity of equilibrium hydrogen plasma at different pressures. *Usual* values for the transport cross sections (solid line: GS; dashed line: CA; dotted line: DH).

The viscosity coefficient behaves essentially like the thermal conductivity of heavy particles. In Fig. 2.4 the plasma viscosity for different plasma pressures as obtained with the three cutoff models is reported. Also in this case, the differences are due to differences in the equilibrium composition. Again at high pressure the viscosity calculated with the ground state method lies between GS and DH methods.

The thermal conductivity of electrons and the electrical conductivity are shown in Figs. 2.5-2.6 respectively. These coefficients depend on electron collisions, therefore the differences of the three models in electron concentration, coupled to the differences between electron-atom and electron-proton cross sections explain the observed results.

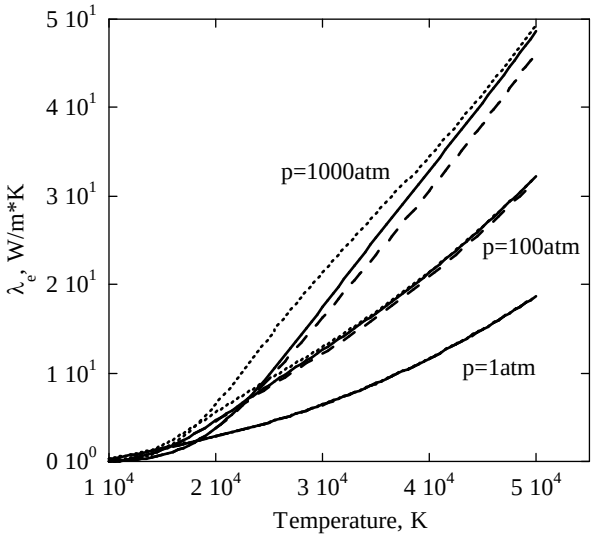

Figure 2.5. Translational thermal conductivity of electrons of equilibrium hydrogen plasma at different pressures. *Usual* values for the transport cross sections (solid line: GS; dashed line: CA; dotted line: DH).

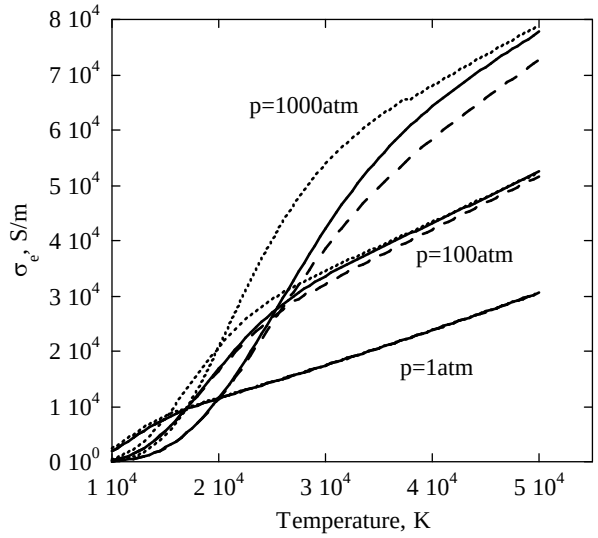

Figure 2.6. Electrical conductivity of equilibrium hydrogen plasma at different pressures. *Usual* values for the transport cross sections (solid line: GS; dashed line: CA; dotted line: DH).

Finally in Figs. 2.7-2.8 we show the reactive thermal conductivity and the internal thermal conductivity of all components. Also in this case the cut-off criterion used in the calculation of equilibrium composition and of thermodynamic properties entering in the relevant equations for internal and reactive contribution determines strong differences in these transport coefficients.

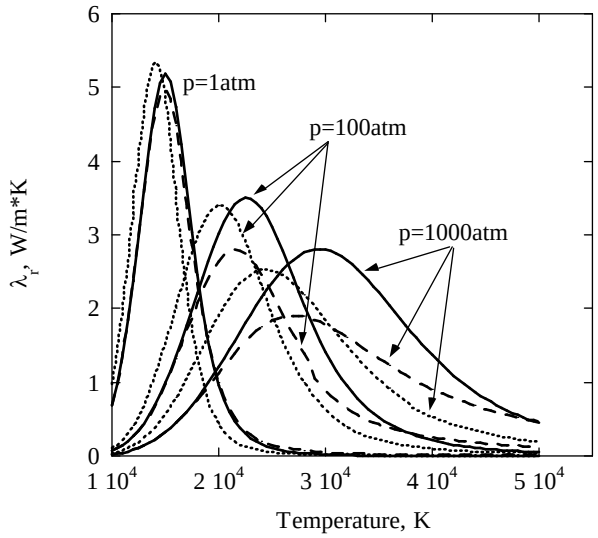

Figure 2.7. Reactive thermal conductivity of equilibrium hydrogen plasma at different pressures. *Usual* values for the transport cross sections (solid line: GS; dashed line: CA; dotted line: DH).

In particular the inclusion of the lowering of ionization potential in DH method is such to anticipate the maximum in the reactive thermal conductivity as compared with the corresponding results obtained with GS and CA methods (see Fig.2.7). On the other hand GS and CA methods present maxima in the reactive thermal conductivity located approximately at the same temperature. Moreover the maximum occurring in the GS method is much higher than the corresponding maximum of the CA method. This is the consequence of the fact that the ΔH of the ionization reaction: $H(n) = H^+ + e$, appearing in the reactive thermal conductivity is higher in the GS method compared with the corresponding quantity obtained by the CA method.

Concerning the internal contributions calculated according CA and DH methods, we can note that they present a trend similar to that one discussed for the reactive thermal conductivity (the internal thermal conductivity in the GS method is zero for definition). Again the maximum in the DH method anticipates that one of CA method presenting at the same time smaller values as a result of the minor number of levels inserted in the electronic partition function and in their internal specific heats. It is also worth noting that the differences in the two methods increase with pressure.

As a whole these results confirm and extend earlier results describing the dependence of transport coefficients on the cut-off criterion used for terminating the electronic partition function in atomic nitrogen plasmas [36].

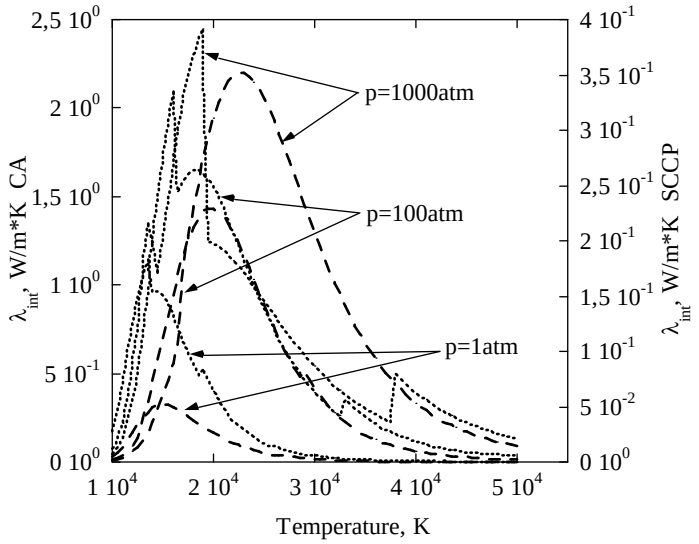

Figure 2.8. Internal thermal conductivity of equilibrium hydrogen plasma at different pressures. *Usual* values for the transport cross sections (dashed line: CA; dotted line: DH).

2.1.3.2 Influence of EES cross sections

The effect of EES on the plasma transport coefficients is due to the large EES collision integrals. The largest increase pertains to H(n)-H^+ diffusion-type collision integrals (Fig. 2.2a) and, to a minor extent, to H(n)-H^+ viscosity-type collision integrals (Fig. 2.2b), whereas H(n)-e show a smaller dependence on the principal quantum number n. The highest effect is therefore expected on the internal and reactive contributions while the translational thermal conductivity of heavy particles as well as the viscosity should be less affected. These effects are then modulated by differences in the atom concentration and in the number of allowed EES predicted by different models. In order to show the relative weight of these effects, the GS model results are taken as benchmark for comparisons. The GS model completely neglects the presence of EES and is therefore not dependent on any assumption about EES cross sections. In the following, the results obtained by using a different cutoff model *and* appropriate EES cross sections (*abnormal* values) are compared for equilibrium atomic hydrogen plasma at different pressures.

Figures 2.9-2.10 report the translational thermal conductivity of heavy particles and the viscosity. In the CA model the differences produced by EES cross sections are very large and overcome the differences introduced by different thermodynamic models. We can note in fact that the CA curves are situated below the corresponding GS ones reversing the behavior shown in Figs. 2.3-2.4. The DH model, instead, predicts larger ionization and smaller number of EES. In particular at high pressure, where the effect of EES should become significant, DH model predicts a large lowering of the ionization potential that affects the

atom concentration together with the number of allowed EES. Thermodynamics prevails on the effect due to abnormal cross sections so in DH model the effect of EES is strongly reduced, never exceeding 5% of the GS value. The differences with Figs. 2.3-2.4 are indeed small.

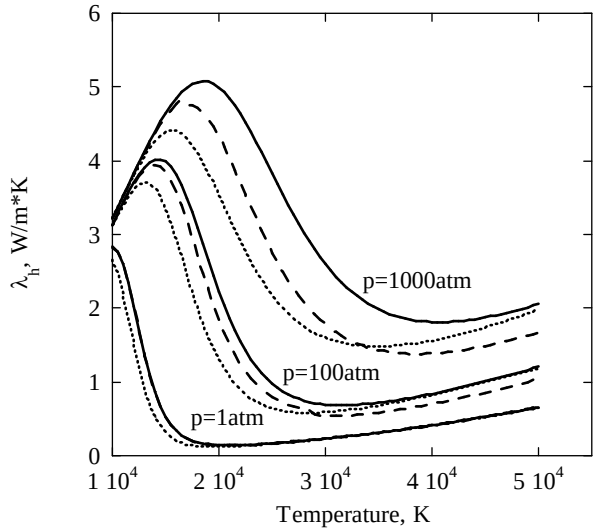

Figure 2.9. Translational thermal conductivity of heavy particles of equilibrium hydrogen plasma at different pressures. *Abnormal* values for the transport cross sections (solid line: GS; dashed line: CA; dotted line: DH).

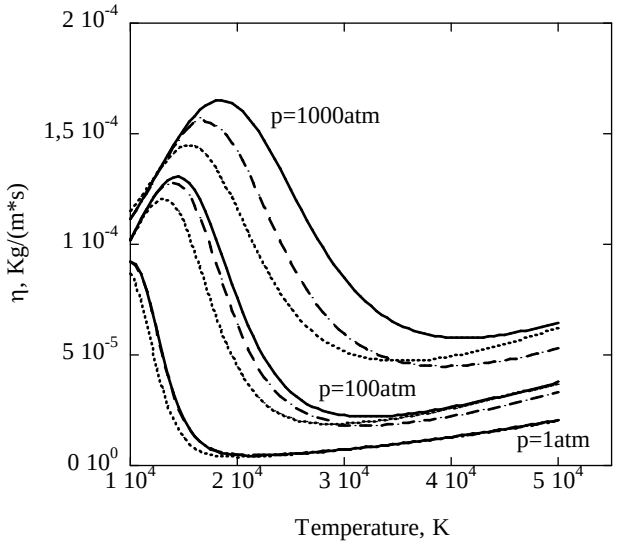

Figure 2.10. Viscosity of equilibrium hydrogen plasma at different pressures. *Abnormal* values for the transport cross sections (solid line: GS; dashed line: CA; dotted line: DH).

The electron transport coefficients weakly depend on EES cross sections and strongly on ionization degree. This is shown in Figs. 2.11-2.12 for the translational thermal conductivity of electrons and the electrical conductivity. Comparison of the relevant curves with the corresponding results reported in Figs. 2.5-2.6 shows the effect of abnormal cross sections specially for the CA method compared with GS one. The effect is indeed very small in the DH model where thermodynamic effects prevail.

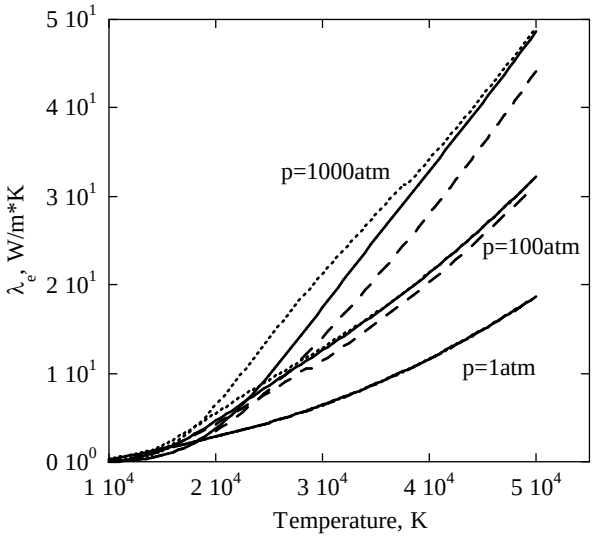

Figure 2.11. Translational thermal conductivity of electrons of equilibrium hydrogen plasma at different pressures. *Abnormal* values for the transport cross sections (solid line: GS; dashed line: CA; dotted line: DH).

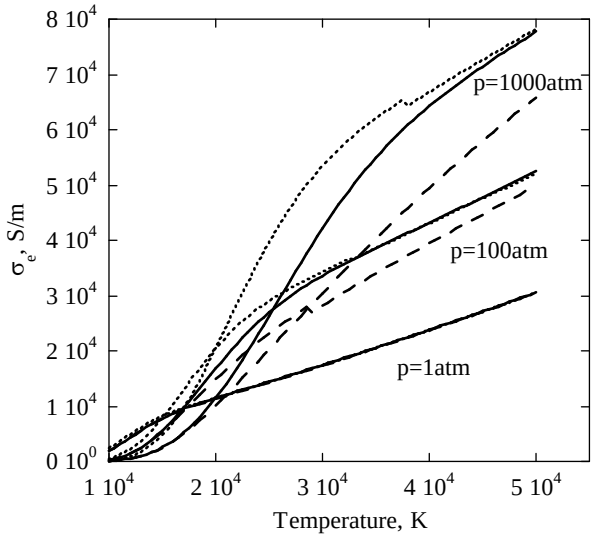

Figure 2.12. Electrical conductivity of equilibrium hydrogen plasma at different pressures. *Abnormal* values for the transport cross sections (solid line: GS; dashed line: CA; dotted line: DH).

Finally in Figs. 2.13-2.14 we report the reactive thermal conductivity and the internal thermal conductivity calculated by using the abnormal cross sections.

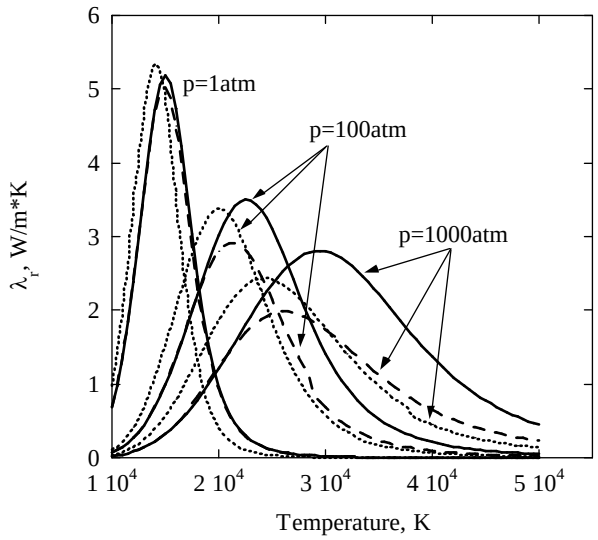

Figure 2.13. Reactive thermal conductivity of equilibrium hydrogen plasma at different pressures. *Abnormal* values for the transport cross sections (solid line: GS; dashed line: CA; dotted line: DH).

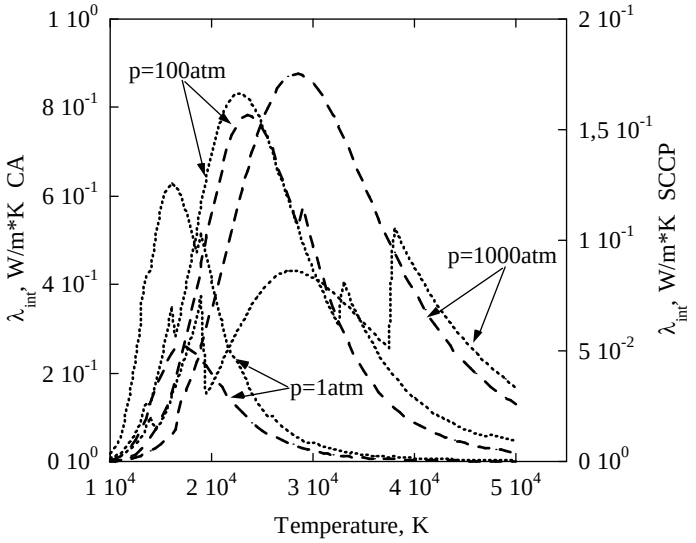

Figure 2.14. Internal thermal conductivity of equilibrium hydrogen plasma at different pressures. *Abnormal* values for the transport cross sections (dashed line: CA; dotted line: DH).

Comparison of the relevant curves of the reactive thermal with the corresponding values of Fig. 2.7 shows that CA results are strongly affected by the insertion of abnormal cross sections, while the DH results are slightly modified. This is indeed due to compensation effects rather than to an insensitivity of the reactive thermal conductivity on the abnormal cross sections.

The situation completely changes for the internal contribution to the thermal conductivity. Comparison of the relevant curves of Fig. 2.14 with the corresponding ones of Fig. 2.8 shows dramatic effects on the influence of the abnormal cross sections in both the results coming from CA and DH methods (see Appendix A for details).

2.2 Air plasmas

Extensive and accurate tabulations of transport coefficients (viscosity, thermal and electrical conductivity) [1,37,38,39] and transport cross sections [40,41] for air plasmas are nowadays available in literature, the excited state issue still represents an open problem. In transport calculations, chemical species are usually regarded as being in the ground state, however a deep investigation on the case of atomic hydrogen plasma reported in section 2.1 has shown that transport coefficients are strongly affected by the presence of electronically excited atoms, especially in high pressure regimes and under the action of an external magnetic field [20]. These results justify the interest for re-evaluation of air plasma transport coefficients including excited states and, in turn, for the extension of existing collision integral database to excited species, i.e. oxygen and nitrogen atoms and ions. Reference it should be done to the pioneering work in this field by different authors [42,43,44,45], attempting the accurate calculation of diffusion and viscosity-type collision integrals for interactions involving the so-called *low-lying* excited states of N and O atoms, i.e. low-energy states characterized by the same electronic configuration of the ground state. Recently a complete revision of old results for oxygen system has been performed [46], based on accurate ab-initio interaction potentials for valence states. The inelastic contribution to odd-order collision integrals due to resonant charge-exchange processes in atom-parent-ion collisions have been evaluated from the corresponding cross sections recalculated in the framework of the asymptotic theory [47,48,49] considering different momentum coupling schemes. An attempt to study the effects of excited species in an LTE nitrogen plasma can be found in recent papers by Aubreton et al. [28,29], however restricted to dissociative regime, i.e. neutral atom interactions. The transport coefficients of an air plasma, in thermodynamic equilibrium, are derived, considering low-lying excited atoms (N^H, O^H) and ions (N^{+H}, O^{+H}) as independent chemical species, characterized through their own transport cross sections. The sensitivity of results to the inclusion of excited states is proven by comparison with the usual ground-state approach. A phenomenological approach [50] is proposed for the calculation of internally consistent and complete data sets of elastic collision integrals for excited-state interactions.

2.2.1 Collision integrals for low-lying excited state

The traditional scheme of collision integral calculation needs the knowledge of accurate potential energy curves for the electronic terms correlating with species in a specific quantum state. In many cases this represents the main difficulty in including excited species, and the reason is that in the composition of orbital and spin angular momenta a multiplicity of states arise, whose potential energy curves are largely unknown. For N_2^H and N_2^{+H} excited systems only few electronic terms are available from ab-initio calculations or from spectroscopic data models, reflecting the theoretical and experimental limits in studying excited states.

The elastic contribution to collision integrals is estimated classically from the interaction potential, φ, adopting a phenomenological approach, already validated in the case of ground state interactions [50]. The proposed approach models the potential, considering the average interaction and resulting from the balance of attractive and repulsive terms [51,52]

$$\varphi(x) = \varepsilon_0 \left[\frac{m}{n(x)-m} \left(\frac{1}{x}\right)^{n(x)} - \frac{n(x)}{n(x)-m} \left(\frac{1}{x}\right)^{m} \right] \tag{2.1}$$

where $x=r/r_e$, $n(x)=\beta+4x^2$. Potential features, as the well depth, ε_0, and well position, r_e, are derived by correlation formulas given in terms of fundamental physical properties of involved interacting partners (polarizability α, charge, number of electrons effective in polarization) [53,54,55,56,57]. The *m* parameter depends on the interaction type (4 for ion-neutral and 6 for neutral-neutral interactions, respectively), while a simple empirical formula, based on polarizability of colliders, has been proposed [50] for the estimation of β parameter, whose values range from 6 to 10 depending on the hardness of interacting

electronic distribution densities. Polarizability values for relevant species are taken from literature [58,59,60]. It should be noted that the potential functional form is the same adopted for describing the interaction between not excited species, this choice is justified considering that low-lying excited states are characterized by physical properties quite similar to the ground state and by small energy separation.

Reduced collision integrals, $\Omega^{(\ell,s)*}$, have been calculated, up to order (4,4), over a wide range of reduced temperatures and fitted as a function of both temperature and β parameter [61], allowing the estimation of collision integrals on the base of the *tuplet* (r_e,ε_0,β,*m*) completely characterizing the physical system.

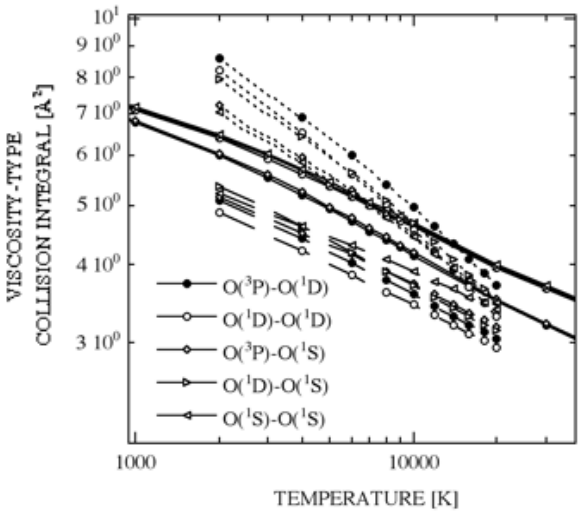

Fig. 2.15. Viscosity-type collision integrals for O-O^H interactions from phenomenological approach (continuous lines), compared with results from Refs. [43] (dashed lines) and [46] (dotted lines).

Viscosity-type collision integrals for O-O^H interactions, obtained with the phenomenological approach, are plotted in Fig. 2.15 together with two series of data available in literature [43,46], based on a multi-potential traditional approach. Being the (2,2) term not affected by resonant excitation-exchange in asymmetric collisions, the observed deviations could give indication of the accuracy of the proposed procedure. A general satisfactory agreement is found between data sets in the considered temperature range [2,000-20,000 K], being the percentage relative error confined below 25% with respect to Ref. [46]. The error analysis should also take into account that the traditional multi-potential procedure, including all electronic-term contributions, is based in Refs. [43,46] on a rigid classification of repulsive (*decaying exponential function*) and bound (*Morse function*) states that could affect data accuracy.

2.2.1.1 Resonant excitation/charge exchange processes

The proposed phenomenological approach does not account for the contributions to odd-ℓ collision integrals coming from inelastic channels, represented by the resonant charge-exchange and excitation-exchange processes occurring in atom-parent-ion and asymmetric atom-atom interactions, respectively. The actual collision integral results from the following relation [62]

$$\Omega^{(\ell,s)*} = \sqrt{\Omega_{el}^{(\ell,s)*} + \Omega_{in}^{(\ell,s)*}} \qquad (2.2)$$

The inelastic term, $\Omega_{in}^{(\ell,s)*}$, is estimated by means of a closed formula, suggested by Devoto [63], for a linear dependence of the square root of charge transfer cross section on the collision velocity, and then fitted with a suitable function of *ln*(T).

For the resonant charge exchange process (Fig. 2.16), occurring in atom-parent ion collisions, reference is made to recent papers by Kosarim and Smirnov [48,49], in which the corresponding cross sections have been derived in the asymptotic theory, considering different momentum coupling schemes, for those interactions, between nitrogen atoms and ions, allowed by single-electron transition.

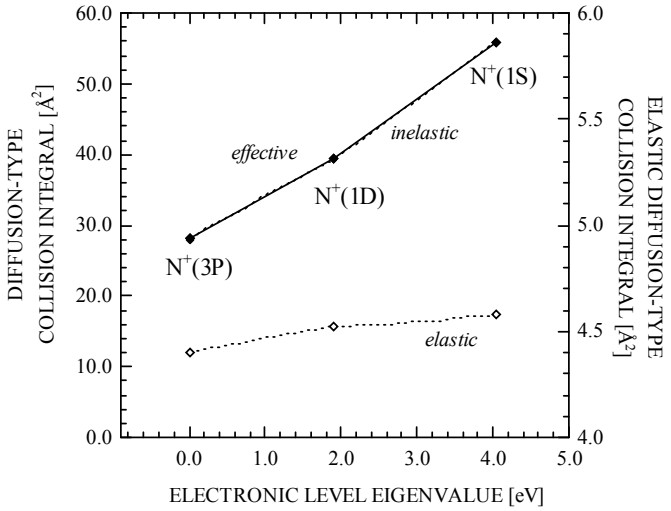

Fig. 2.16. Effective diffusion-type collision integral, with elastic and inelastic components, as a function of quantum state of the ionic collision-partner in $(N^+)^H$-$N(^2P)$ interactions, at T=10,000 K.

Concerning the exchange of excitation in asymmetric collisions between nitrogen atoms, few references can be found in literature [42,28] and it is re-evaluated adopting an asymptotic approach and considering, for these cases of dipole-forbidden electronic transitions, the simultaneous transition of two electrons between the two ionic cores. The exchange interaction has an analytical expression [64], depending on the quantum numbers characterizing the state of valence electrons undergoing the resonant process, and present results are obtained including only terms with null axial projection (ℓ=1,*m*=0), representing the main contribution [65]. This approach predicts higher values than those obtained by the evaluation of gerade-ungerade splitting from potential energy curves [42,28], however the direct estimation could be affected by the lower accuracy characterizing the region of large internuclear distances, where the process takes place favourably. As generally observed, the inelastic contribution is significantly higher with respect to the elastic one, especially in the high temperature region, dominating the temperature-dependence of the diffusion-type collision integral and, consequently, also its dependence on the electronic excitation of colliding partners.

2.2.2 Transport properties

Transport coefficients (*multi-component diffusion coefficients*, D_j^k, *true translational thermal*, λ, *internal*, λ_{int}, and *electrical*, σ_e, *conductivities*) are calculated, in the framework the Chapman-Enskog theory, using, as input data, the recommended collision integral values for ground air species collected in Ref. [66] and, for low-lying excited states of atomic oxygen and nitrogen, the dynamical data discussed in the previous section. Where no state-dependent collision integrals are available, as for electron-atom interactions, it is assumed that their values are equal to ground-state case ($\sigma^2\Omega_{e-N^*}^{(\ell,s)*} = \sigma^2\Omega_{e-N}^{(\ell,s)*}$,

$\sigma^2\Omega^{(\ell,s)*}_{e-O^*} = \sigma^2\Omega^{(\ell,s)*}_{e-O}$).

The third Chapman-Enskog approximation has been used throughout in order to provide accurate results also in the ionization regime.

The equilibrium composition of the 19-ground-species air plasma ($N(^4S)$, $O(^3P)$, N_2, O_2, NO, $N^+(^3P)$, N^{2+}, N^{3+}, N^{4+}, $O^+(^4S)$, O^{2+}, O^{3+}, O^{4+}, O^-, N_2^+, O_2^+, O_2^-, NO^+, e) is determined as a function of temperature, at atmospheric pressure, by using a hierarchical algorithm, recently reconsidered in Ref. [67]. The equilibrium assumption leads to excited state population densities governed by the corresponding term in the Boltzmann distribution.

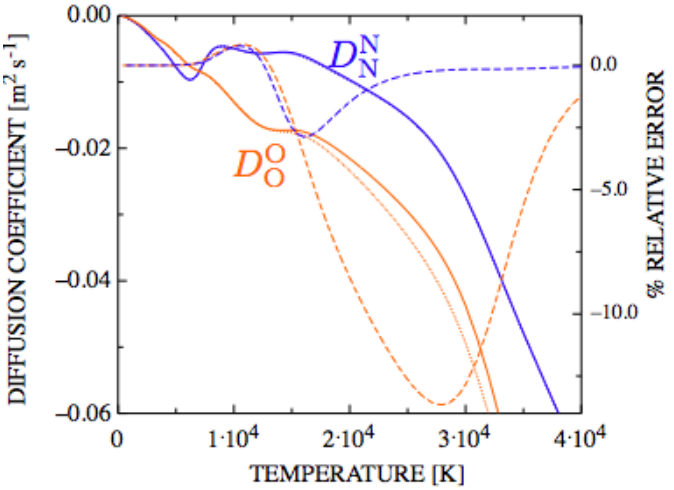

Fig. 2.17. Self diffusion coefficients of nitrogen and oxygen atoms, as a function of temperature. case (a)-(continuous lines), case (b)-(dotted lines), percentage relative error-(dashed lines).

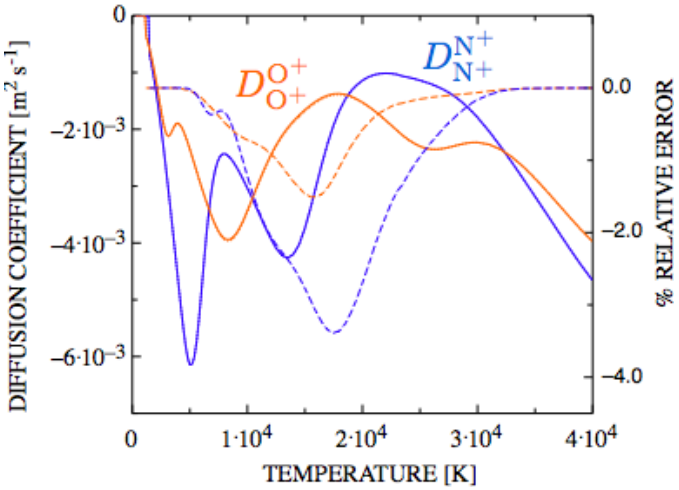

Fig. 2.18. Self diffusion coefficients of nitrogen and oxygen ions, as a function of temperature. case (a)-(continuous lines), case (b)-(dotted lines), percentage relative error-(dashed lines).

In order to investigate the role of electronically excited states in determining transport coefficients, two cases are considered

- case (a) collision integrals for excited-species interactions are set equal to the corresponding ground state value (27 species)
- case (b) low-lying excited states for ions and atoms are included with their own collision integral values (27 species)

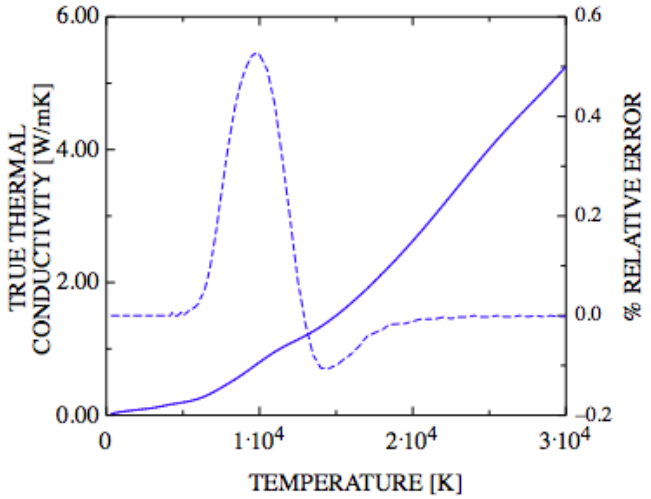

Fig. 2.19. True translational thermal conductivity as a function of temperature, neglecting [case (a)-(continuous line)] or including [case (b)-(dotted line)] low-lying excited states, with percentage relative error-(dashed line).

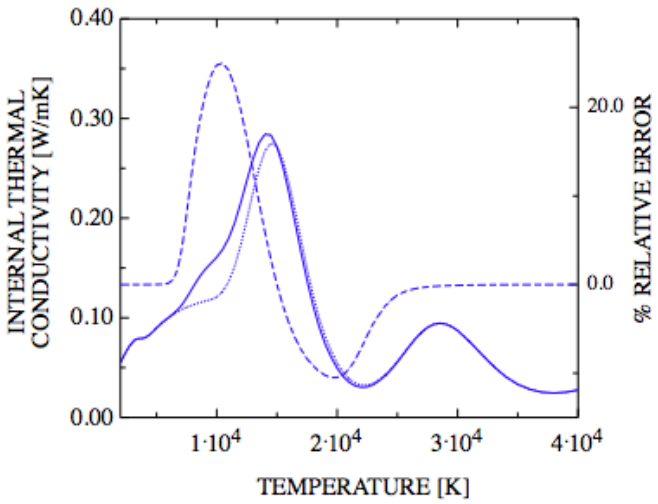

Fig. 2.20. Internal thermal conductivity as a function of temperature, neglecting [case (a)-(continuous line)] or including [case (b)-(dotted line)] low-lying excited states, with percentage relative error-(dashed line).

Figs. 2.17-2.18 display the temperature dependence of selected self-diffusion coefficients in the two cases. The percentage relative error, defined as 100 [case (a)-case (b)]/case (a) is also reported. Deviations are found in the [15,000-30,000 K] interval, corresponding to the appearance of ionic species in the plasma, where the diffusion is governed by charge exchange processes. The true translational thermal conductivity (Fig. 2.19) shows differences in the temperature region where excited atoms exist, while the effect is lower in ionization regime. Differently the internal thermal conductivity value is significantly modified by excited-state inclusion (Fig. 2.20) in the whole temperature range, with extrema of the percentage relative error localized at temperatures corresponding to the existence of excited atoms and ions. In particular we

can note that the used of actual transport cross sections decreases the internal thermal conductivity of 35% at 10,000 K as compared with ground state transport cross sections. Finally Fig. 2.21 reports the role of low-lying excited states on the viscosity; differences in this case do not exceed 6%.

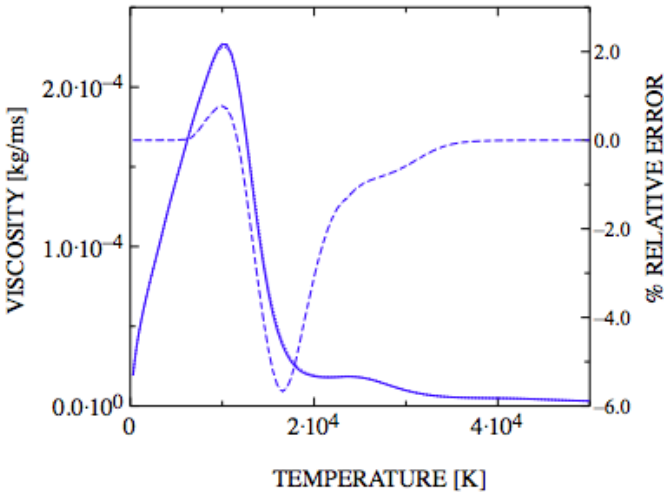

Fig. 2.21. Viscosity as a function of temperature, neglecting [case (a)-(continuous line)] or including [case (b)-(dotted line)] low-lying excited states, with percentage relative error-(dashed line).

Significant departures are therefore observed from results obtained by using the usual approach, confirming the not negligible role of excited states, that are more effective in collisions, being, in general, characterized by higher cross sections. An increase of the pressure should emphasize the effects, because it acts shifting the ionization equilibrium to higher temperatures and favouring the population of excited states, however the system is sensitive even at p=1 atm, due to the small level energy separation. Presented results do not account for high-lying excited states of atomic species, whose collision integrals are expected to exhibit a strong dependence on the principal quantum number of the valence electrons, as demonstrated in the case of the $\sigma^2\Omega_{in}^{(1,1)*}$ for atom-parent-ion interactions [47] (see Fig. 2.22). These states should strongly affect the transport coefficients of air plasmas for T>10,000 K.

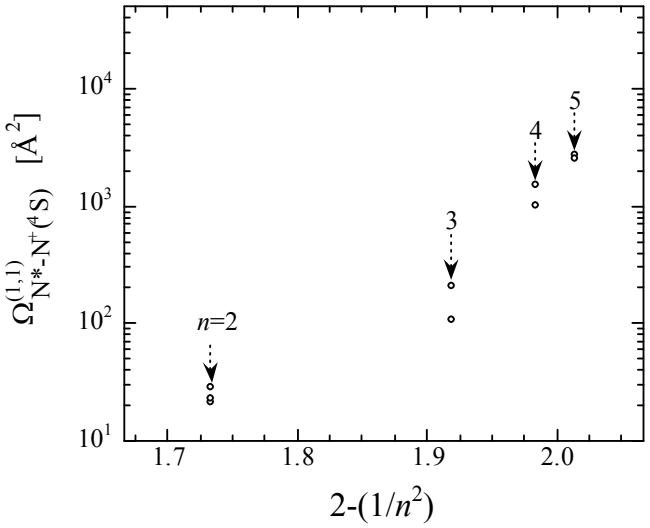

Fig. 2.22. Dependence of diffusion-type collision integrals for the interaction $N^+(^3P)$-N on the principal quantum number of the atom valence shell electrons, *n*, at T=10000 K (different electronic states of N, arising from the same electronic configuration have been considered. *n*=2 $N(2p^3\ ^4S,^2D,^2P)$, *n*=3 $N(2p^23s\ ^2P,^4P;)$, *n*=4 $N(2p^24s\ ^2P,^4P;)$, *n*=5 $N(2p^25s\ ^2P,^4P;)$.

CONCLUDING REMARKS

In this lecture we have emphasized the role of electronically excited states in affecting the thermodynamic properties of high-temperature-high-pressure thermal plasmas. Detailed thermodynamic results have been reported for hydrogen and nitrogen plasmas. In both cases we have observed strong compensation effects between frozen and reactive contributions to the total specific heat. In particular the excited states strongly increase the frozen specific heat as compared with the ground-state method, having an opposite effect on the reactive contribution. This kind of compensation hides the importance of electronically excited states in affecting the total thermodynamic properties of thermal plasmas. This consideration is valid for atomic hydrogen plasma and for nitrogen plasma in the temperature range where the first two ionization equilibria exist. The situation completely changes at the onset of the third and fourth ionization equilibria. Another interesting aspect is the effect of electronically excited states on the dissociation equilibrium of N_2 plasma. In this case comparison of the specific heat calculated including and neglecting the so-called low-lying excited states for both atoms and molecules shows non-negligible differences which increase with pressure. It should be also stressed the role of the choice of energy levels (Coulomb, Debye-Hückel) in affecting the thermodynamic properties of atomic hydrogen plasma. Similar trends occur for the isentropic coefficients of hydrogen and nitrogen plasmas.

The role of electronically excited states in affecting the transport properties of thermal plasmas has been investigated for both hydrogen and air plasmas. The previous differences observed for hydrogen thermodynamic properties propagate in transport coefficients when all the excited states are considered as having the same transport cross section as the ground state. The situation becomes more complex when inserting state-to-state cross sections, i.e. transport cross sections depending on the principal quantum number. This aspect has been fully considered for atomic hydrogen plasma, where we have shown important effects on transport coefficients. Once again due to mixed terms in the Chapman-Enskog theory internal and reactive contributions to the total thermal conductivity of the plasma present compensation effects similar to those described for thermodynamic properties. The situation for air plasmas is discussed especially from the point of view of transport cross sections of low-lying excited states. Extensive data sets of collision integrals have been tabulated in our group and used to clarify the influence of low-lying excited states on the transport coefficients of atmospheric air plasmas. The results show a non-negligible role of these states in determining multi-component diffusion coefficients as well as internal thermal conductivity and viscosity. Work is in progress to understand high-lying excited states as in the case of atomic hydrogen plasmas.

As a whole we can conclude that electronically excited states play an important role in affecting thermodynamic and transport properties of thermal plasmas. The complete solution of this problem needs an unique cut-off criterion of partition function as well as a reliable data set of high-lying transport cross sections for air plasmas.

APPENDIX A TRANSPORT OF INTERNAL AND REACTIVE ENERGY

The transport of vibrational and rotational internal energy is an important mechanism for increasing the thermal conductivity of diatomic and polyatomic molecules. Different theories have been proposed, the most simple being represented by the Eucken theory [68]. In this case the rotational and vibrational contributions to the thermal conductivity can be obtained by the following equation:

$$\lambda_{\text{Rot+Vib}} = \eta \cdot (c_{V,\text{Rot}} + c_{V,\text{Vib}}) \tag{A.1}$$

where η is the shear viscosity coefficient and $c_{V,\text{Rot}}$ and $c_{V,\text{Vib}}$ are the contribution of rotational and vibrational degrees of freedom to the constant volume specific heat. More precisely the Chapman-Enskog method gives for a simple gas [69]:

$$\lambda_{\text{Rot+Vib}} = \rho\mathcal{D} \cdot (c_{V,\text{Rot}} + c_{V,\text{Vib}}) \tag{A.2}$$

where ρ is the mass density and $\mathcal{D}$ is the self-diffusion coefficient.

Equation (A.2) coincides with Eq. (A.1) in the following approximation:

$$\frac{\rho\mathcal{D}}{\eta} = 1 \tag{A.3}$$

Equation (A.2) results from the following assumptions:

- Boltzmann distribution over internal states;
- Independence of internal states and molecular velocity;
- Inelastic collisions are negligible;
- Cross sections do not depend on the internal state.

Improvement of this simple theory has been obtained by including the effect of inelastic collisions [70,71] as well as the effect of non-equilibrium vibro-rotational distribution functions [72]. These studies basically confirm the Eucken approach.

On the contrary, the transport of electronic energy due to the diffusion of electronically excited states is usually neglected on the believe that the electronic energy content is usually small and that the diffusion cross sections of electronically excited states are very high. On the basis of these arguments Devoto concluded many years ago that the transport of electronic energy could be neglected in local thermodynamic equilibrium (LTE) plasmas [73]. Devoto used the simple Eucken expression, Eq. (A.2), that is reported here specialized for the electronic degrees of freedom:

$$\lambda = \lambda_{\text{tr}} + \lambda_{\text{E}} = \tfrac{5}{2}\eta c_V \left\{ 1 - \left(1 - \frac{2}{5}\frac{\rho\mathcal{D}}{\eta} \right) \frac{c_{V,\text{E}}}{c_V} \right\} \tag{A.4}$$

where c_V is the total specific heat.

An estimation of the term $\rho\mathcal{D}/\eta$ for hydrogen gives a value of about 0.5 while $c_{V,\text{E}}$ m/k was estimated to lie in the interval $1.34\ 10^{-4}$ - $4.7\ 10^{-2}$ in the temperature range 8,000-15,000 K, considering the effect of only the first electronic state of atomic hydrogen. This simple estimation does not consider that in thermal plasmas, depending on the pressure and on the temperature, the adimensional internal specific heat can

reach values up to 10-100 so that the second term in Eq. (2.4) can be more important than the translational contribution. Of course this dramatic increase of internal specific heat is due to the excitation of electronically excited states belonging to very high principal quantum numbers so that also the rough estimation of the factor $\rho\mathcal{D}/\eta$ performed by Devoto should be improved. These considerations have never been taken into account so that the contribution of the electronic degrees of freedom to the thermal conductivity has been completely overlooked.

In addition, since the excitation of electronic states occurs in the same temperature range as the ionization process, the transport of ionization energy is a strictly correlated phenomenon to which we now turn. For atomic plasmas it can be calculated through the equation [74]:

$$\lambda_r = p\frac{\Delta H^2}{k^2 T^3}\frac{N_e N_H}{(N_e+N_H)^2}\mathcal{D}_H^{H^+} \tag{A.5}$$

where N_i are number densities, $\mathcal{D}_H^{H^+}$ is the atom-proton binary diffusion coefficient [69] and ΔH is the reaction enthalpy:

$$\Delta H = \frac{5}{2}kT + I - E_H \tag{A.6}$$

Here, I is the ionization potential eventually corrected by its lowering due to the microfields, 5/2kT is the translational enthalpy and E_H is the internal electronic energy of atomic hydrogen. According to these equations, internal energy content contributes to decrease the transport of ionization energy; in other words, electronic excitation can paradoxically decrease the diffusive transport in thermal plasmas.

Additionally, many years ago [75] it was found, and confirmed more recently [25], that the transport of ionization energy in atomic LTE plasmas is almost independent of the presence of electronically excited states which, with their enormous charge transfer cross sections, should decrease the corresponding contribution. The reactive thermal conductivity at atmospheric pressure is left unchanged when taking into account and neglecting the dependence of electronically excited cross sections on the principal quantum number. This puzzling behavior was ascribed to some compensation effects present in the determinantal equation describing the reactive thermal conductivity.

The maximum number of allowed EES is determined by the confined atom (CA) model:

$$a_0 n_{max}^2 < N^{-1/3} \tag{A.7}$$

where a_0 is the Bohr radius, n_{max} the maximum allowed principal quantum number and N the particle density. The number of EES actually used in calculations, however, never exceeds 12 due to the poor knowledge of collision integral data for hydrogen atoms with larger principal quantum number. This restriction only affects calculations at p=1 atm where $n_{max} = 12$ is used throughout.

Calculations are carried out to the second non-vanishing approximation in Sonine polynomials. The collision integrals for the relevant interactions among H(n), H^+ and electrons present a strong dependence on the principal quantum number especially for collision integrals diffusion-type of H(n)-H^+ collisions (fig. 2.2a). It is worth noting that the collision integrals adopted in this work describe only elastic and charge transfer processes. Other inelastic and reactive processes are completely neglected on the believe that they do not affect significantly the results. While this approach is certainly justified for inelastic processes [70,71] its extension to reactive processes is open to question [76].

The convective heat flux describes the transport of enthalpy due to diffusion. It is defined by:

$$\mathbf{q} = \sum_i N_i h_i \mathbf{V}_i = -(\lambda_r + \lambda_{int}) \cdot \nabla T \tag{A.8}$$

where h_i is the enthalpy carried by *i*-type particles, $\mathbf{V}_i$ the diffusion velocity and λ_r, λ_{int} are the reactive and internal thermal conductivity, respectively.

It is further assumed that [77]:

- thermal diffusion is negligible;
- total pressure is uniform;
- there are not non-electromagnetic forces acting on the plasma;
- the plasma is quasi neutral;
- the plasma is in thermal and chemical equilibrium;
- the total current density equals zero (i.e. the ambipolar diffusion regime has been established, as in all actual experiments).

Under these assumptions, the diffusion velocities read:

$$\mathbf{V}_i = -\sum_j D_{ij} \mathbf{d}_j \tag{A.9}$$

where:

$$\mathbf{d}_i = \nabla\left(\frac{N_i}{N}\right) - \frac{N_i}{N}\frac{e_i \mathbf{E}'}{kT} \tag{A.10}$$

and $\mathbf{E}'$ is the ambipolar electric field.

In particular, in Eq. (A.9) the sum over atomic levels read:

$$\sum_{n=1}^{n_{max}} D_{in} \mathbf{d}_n = D_{iH} \mathbf{d}_H + \sum_{n=1}^{n_{max}} \frac{N_n}{N} D_{in} \frac{E_n - E_H}{kT^2} \nabla T \tag{A.11}$$

The gradients of the species concentrations are then expressed in terms of the equilibrium constant and the ambipolar electric field in terms of the gradient of the temperature [77].

Now, the second term on the RHS. of Eq. (A.11) does not vanish also in the case that no chemical reaction occurs and it is therefore recognized as the term producing the internal thermal conductivity. It is also worth pointing out that the approach used in Ref. [25] combines these two contributions into a single thermal conductivity coefficient. The reactive conductivity discussed in that work, therefore, includes also the contribution from the transport of electronic excitation energy.

The assumption of equal cross sections for all EES being no longer valid, the question arises what the effect will be on the transport of electronic and ionization energy. In a previous work [25] the internal and reactive contributions were mixed together and the overall effect was barely noticeable. We wish to show that, indeed, the effect of EES is by no means negligible and that it produces in the two coefficients modifications of opposite sign that compensate in the thermal equilibrium case. This realization is useful in that, if the equilibrium condition is relaxed (it is often the case for low-temperature discharge plasmas) large influence of EES on transport of electronic and ionization energy can be expected.

In order to understand how the EES cross sections affect these coefficients rewrite the convective heat flux, Eq. (A.8) as:

$$q_{r+int} = N_e \tfrac{5}{2} kT \mathbf{V}_e + N_e \left(\tfrac{5}{2} kT + I\right) \mathbf{V}_e + \sum_n N_n \left(\tfrac{5}{2} kT + E_n\right) \mathbf{V}_n \tag{A.12a}$$

$$\sum_n N_n \left(\tfrac{5}{2} kT + E_n\right) \mathbf{V}_n = \left(\tfrac{5}{2} kT + E_H\right) \cdot n_H \mathbf{V}_H + \sum_n N_n \left(E_n - E_H\right) \mathbf{V}_n \tag{A.12b}$$

The diffusion velocities are made up of two contributions:

$$\mathbf{V}_j = \underbrace{-D_{je}\mathbf{d}_e - D_{jH^+}\mathbf{d}_{H^+} - D_{jH}\mathbf{d}_H}_{\mathbf{z}_j} \underbrace{- \sum_{n=1}^{n_{max}} \frac{N_n}{N} D_{jn} \frac{E_n - E_H}{kT^2} \nabla T}_{\mathbf{y}_j} \tag{A.13}$$

Recalling that:

$$\mathbf{V}_i = \mathbf{V}_e \tag{A.14}$$

and:

$$\sum_n N_n \mathbf{V}_n = N_H \mathbf{V}_H \approx -N_e \mathbf{V}_e \tag{A.15}$$

we arrive at:

$$\mathbf{q}_{int} = \underbrace{N_e \mathbf{y}_e \tfrac{5}{2} kT}_{i1} + \underbrace{N_e \mathbf{y}_{H^+} \left(I - E_H\right)}_{i2} + \underbrace{\textstyle\sum_n N_n \left(E_n - E_H\right) \mathbf{y}_n}_{i3} \tag{A.16}$$

$$\mathbf{q}_r = \underbrace{N_e \mathbf{z}_e \tfrac{5}{2} kT}_{r1} + \underbrace{N_e \mathbf{z}_{H^+} \left(I - E_H\right)}_{r2} + \underbrace{\textstyle\sum_n N_n \left(E_n - E_H\right) \mathbf{z}_n}_{r3} \tag{A.17}$$

A.1 Internal thermal conductivity

If equal cross sections are considered for all EES:

$$\sum_{n=1}^{n_{max}} \frac{N_n}{N} D_{in} \frac{E_n - E_H}{kT^2} = \begin{cases} 0 \quad ; \quad i = H^+, e \\ \left(D_{ii} - D_{ij}\right) \dfrac{N_i}{N} \dfrac{E_i - E_H}{kT^2} \quad ; \quad \begin{matrix} i = n \,;\, n = 1,\ldots,n_{max} \\ j = m \,;\, m \neq n \end{matrix} \end{cases} \tag{A.18}$$

that gives for the internal thermal conductivity:

$$\boldsymbol{\lambda}_{int} = \frac{N_H}{N} \left(D_{HH} - D_{nm}\right) N_H c_{V,E} \quad ; \quad \begin{cases} n = 1,.. n_{max} \\ m \neq n \end{cases} \tag{A.19}$$

where $c_{V,E} = \dfrac{\left\langle E_n^2 \right\rangle - E_H^2}{kT^2}$ is the internal specific heat per particle.

Eq. (A.19) is the extension of Eucken formula to a multi-component mixture. In the usual case, therefore, the internal thermal conductivity is proportional to the internal specific heat. As mentioned in the introduction the latter can be a considerable fraction of the total plasma specific heat [17].

Figure A.1 shows the internal thermal conductivity of equilibrium hydrogen plasma at different pressures, calculated with ("*abnormal*") and without ("*usual*") different cross sections for EES. It increases with increasing pressure as the population of EES increases and it becomes of comparable value as the reactive term at high pressure. Note that the effect of EES cross sections on this coefficient can be dramatic. Figure A.1, however, shows also some puzzling features: the increase of some cross sections should decrease the diffusion coefficients. According to Eq. (A.19), the abnormal internal thermal conductivity should be correspondingly smaller. The effect of EES cross sections, instead, is to reduce the coefficient below the usual value at low temperatures and above it at high temperatures.

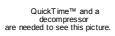

Figure A.1. Internal thermal conductivity of equilibrium hydrogen plasma at different pressures (solid line: abnormal; dashed line: usual).

In order to understand these features rewrite Eq. (A.16) for the usual case:

$$\mathbf{q}_{int} = \sum_n N_n (E_n - E_H)\mathbf{y}_n \qquad (A.20)$$

This is obviously equivalent to Eq. (A.19): the internal thermal conductivity corresponds to the Eucken formula (i.e.: self diffusion times internal specific heat).

In the abnormal case this term is lower due to the large EES cross sections that make the diffusion velocities of high EES smaller. This effect is however counterbalanced by the presence of the terms *i1* and *i2* in Eq. (A.16), which are absent in the usual case. These additional terms read:

$$N_e \mathbf{y}_e \tfrac{5}{2} kT + N_e \mathbf{y}_{H^+} (I - E_H) = \frac{N_e}{N} \sum_n N_n (E_n - E_H) \frac{D_{en} \tfrac{5}{2} kT + D_{H^+ n} (I - E_H)}{kT^2} \nabla T \qquad (A.21)$$

In this formula, all diffusion coefficients are negative and low-lying levels ($E_n < E_H$) give a positive contribution; the diffusion coefficients of higher levels are smaller (in absolute value) with respect to the usual case so that overall the term increases the internal conductivity: the electronic energy of high levels, not being diffused away, acts as if the internal specific heat had increased.

At high temperature, when the ionization fraction is large, this effect can become dominant and the abnormal coefficient is greater than the usual one. The different contributions to the internal thermal conductivity of equilibrium hydrogen plasma are reported in Figs. A.2a,b for two plasma pressures.

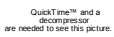

Figure A.2a. Different contributions to internal thermal conductivity of equilibrium hydrogen plasma at p=1 atm (solid line: *abnormal*; dots: *i3*; crosses: *i1+i2*; dashed line: *usual*).

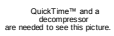

Figure A.2b. Different contributions to internal thermal conductivity of equilibrium hydrogen plasma at p=1000 atm (solid line: *abnormal*; dots: *i3*; crosses: *i1+i2*; dashed line: *usual*). A.2 Reactive thermal conductivity

Figure A.3 shows the reactive thermal conductivity of equilibrium hydrogen plasma at different pressures. The two sets of curves refer to "*usual*" and "*abnormal*" values.

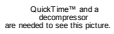

Figure A.3. Reactive thermal conductivity of equilibrium hydrogen plasma at different pressures (solid line: *abnormal*; dashed line: *usual*).

We note that:

- the reactive thermal conductivity decreases with increasing pressure. This happens because at higher pressure ionization shifts to higher temperatures where the term $\Delta H/(kT^2) = (I + \frac{5}{2}kT - E_H)/(kT^2)$ is lower;
- although the EES cross sections are larger than the ground state ones, the abnormal coefficient can be larger than the usual one;
- the coefficient is not dramatically dependent on EES cross sections even at high pressure, when the population of EES is significant;

Overall, the curves follow the behavior predicted by Eq. (A.5) and peak when the reaction has the maximum temperature gradient.

In the usual case, $\mathbf{y}_e = \mathbf{y}_{H^+} = 0$, $\mathbf{z}_e = \mathbf{V}_e = \mathbf{V}_{H^+} = \mathbf{z}_{H^+}$ and r3=0 so that:

$$\mathbf{q}_r = N_e \mathbf{V}_e \Delta H \tag{A.22}$$

The reactive thermal conductivity can therefore be seen as the reaction enthalpy carried by the ion diffusion, in accord with Butler and Brokaw expression, Eq. (A.5). In the abnormal case this term is suppressed due to the increase of atom-proton cross sections. From inspection of Eq. (A.13) we also note that, for each given species j, $\mathbf{z}_j$ has a weaker dependence on EES compared to $\mathbf{y}_j$. In $\mathbf{z}_j$, in fact, atomic diffusion enters through:

$$D_{jH} = \sum_{n=1}^{n_{max}} \frac{N_n}{N} D_{jn} \tag{A.23}$$

In $\mathbf{y}_j$, instead, atomic diffusion is weighted with the energy content of each state: the importance of high-lying levels is therefore increased.

In the abnormal case, in addition, the term r3 does not vanish and balances the previous effect so that the overall effect is small. This latter term describes the difference of the actual atomic diffusion with respect to the average term $N_H E_H \mathbf{z}_H = -N_e E_H \mathbf{z}_{H^+}$. Higher levels diffuse with lower velocity, since have higher cross sections and their contribution to r3 is smaller than in the usual case. This unbalance causes the sum not to vanish. As a result, an effective atomic energy is transported, which is less than the actual one (and the transported reaction enthalpy thus bigger). At its maximum, this effect can be more important than the decrease due to smaller ionic diffusion and the abnormal coefficient is bigger than the usual one. At high temperature, when the atomic fraction becomes small, the first effect dominates again. Figs. A.4a-b illustrate this by comparing the different contributions to the reactive thermal conductivity for the abnormal and usual cases at two different pressures.

The extent to which EES cross sections affect the calculation of the convective contribution (internal and reactive) to the thermal conductivity in atomic hydrogen thermal plasmas is summarized in Fig. A.5 that reports the percentage relative difference between abnormal and usual values of this quantity, normalized to the abnormal value, for different plasma pressures.

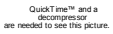

Figure A.4a. Different contributions to reactive thermal conductivity of equilibrium hydrogen plasma at p=1 atm. In this plot the usual and abnormal values are indistinguishable (solid line: *abnormal*; dots: *r1+r2*; crosses: *r3*; dashed line: *usual*).

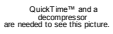

Figure A.4b. Different contributions to reactive thermal conductivity of equilibrium hydrogen plasma at p=1000 atm (solid line: *abnormal*; dots: *r1+r2*; crosses: *r3*; dashed line: *usual*).

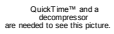

Figure A.5. Percentage relative difference between abnormal and usual values of convective (internal and reactive) thermal conductivities for equilibrium hydrogen plasma at different pressures.

The results of the present work can be therefore summarized as follows:

- the internal thermal conductivity due to atomic electronic energy is a considerable fraction of the convective thermal conductivity, this ratio increasing with pressure;
- EES cross sections affect in a dramatic and non trivial way both the internal and reactive thermal conductivities;
- the changes produced by EES cross sections affect the two coefficients in opposite ways so that the changes on their sum are somewhat reduced. This, in particular, explain the partial compensation apparent in the results of Ref. [25].

These features are clearly visible in Fig. A.6 that reports the percentage relative difference between abnormal and usual values of internal and reactive thermal conductivities and their sum for equilibrium hydrogen plasma at different pressures. The differences are normalized to the abnormal value of the total thermal conductivity (i.e. translational of electrons and heavy particles, internal and reactive contributions) and thus give indications on the real weight of EES cross sections on the properties of thermal plasmas.

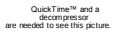

Figure A.6a. Percentage relative difference between *abnormal* and *usual* values of internal and reactive thermal conductivities and their sum for equilibrium hydrogen plasma at p=1 atm (solid line: internal + reactive; dashed line: internal; dotted line: reactive).

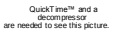

Figure A.6b. Percentage relative difference between *abnormal* and *usual* values of internal and reactive thermal conductivities and their sum for equilibrium hydrogen plasma at p=1000 atm (solid line: internal + reactive; dashed line: internal; dotted line: reactive).

ACKNOWLEDGMENTS

The present work has been partially supported by MIUR PRIN 2007 (2007H9S8SW_003).

REFERENCES

[1] A. D'Angola, G. Colonna, C. Gorse, M. Capitelli, *European Physics Journal D* **46** (2008) 129

[2] T. Magin, G. Degrez, I. Solokova, AIAA Paper 2002-2226, 33rd AIAA Plasmadynamics and Laser Conference, Maui, HI, May 20-23 2002

[3] M.R. Zaghloul, *IEEE Transactions on Plasma Science* **33** (2005) 1973

[4] P. André, W. Bussière, D. Rochette, *Plasma Chemistry and Plasma Processing* **27** (2007) 381

[5] P. Krenec, *Plasma Chemistry and Plasma Processing* **28** (2008) 107

[6] A. Nayfonov, A. Däppen, *Astrophysical Journal* **499** (1998) 489

[7] D. Giordano, M. Capitelli, *Physical Review E* **65** (2001) 016401

[8] V. Rat, J. Aubreton, M.F. Elchinger, P. Fauchais, A.B. Murphy, *Physical Review E* **66** (2002) 056407

[9] V. Rat, J. Aubreton, M. F. Elchinger, P. Fauchais and A. Lefort, *Physical Review E* **64** (2002) 026409

[10] W. Ebeling, M. Steimberg, J. Ortner, *European Physics Journal D* **12** (2000) 513

[11] X. Chen, P. Han, *Journal of Physics D* **32** (1999) 1711

[12] F.J. Rogers, A. Nayfonov, *Astrophysical Journal* **576** (2002) 1064

[13] F.J. Rogers, *Physics of Plasmas* **7** (2000) 51

[14] V.K. Gryaznov, S.V. Ayukov, V.A. Baturin, I.L. Iosilevskly, A.N. Starostin, V.E. Fortov, *Journal of Physics A* **39** (2006) 4459

[15] M. Lisal, W.R. Smith, I. Nezbeda, *Journal of Chemical Physics* **113** (2000) 4885

[16] F. De Palma, A.R. Casavola, M. Capitelli, *Journal of Thermophysics and Heat Transfer* **20** (2006) 921

[17] M. Capitelli, I. Armenise, D. Bruno, M. Cacciatore, R. Celiberto, G. Colonna, O. De Pascale, P. Diomede, F. Esposito, C. Gorse, K. Hassouni, A. Laricchiuta, S. Longo, D. Pagano, D. Pietanza, M. Rutigliano, *Plasma Sources Science and Technology* **16** (2007) S30

[18] M. Capitelli, D. Giordano, G. Colonna, *Physics of Plasmas* **15** (2008) 82115

[19] D. Bruno, M. Capitelli, C. Catalfamo, A. Laricchiuta, *Physics of Plasmas* **14** (2007) 072308

[20] D. Bruno, A. Laricchiuta, M. Capitelli, C. Catalfamo, *Physics of Plasmas* **14** (2007) 022303

[21] H.R. Griem, *Physical Review* **128** (1962) 997

[22] H.R. Griem, "*Principles of Plasma Spectroscopy*" (Cambridge University Press, Cambridge, 1997)

[23] K.M. Roussel, R.F. O'Connell, *Physical Review A* **9** (1974) 52

[24] M. Capitelli, E. Ficocelli, *Journal of Plasma Physics* **5** (1971) 115

[25] M. Capitelli, R. Celiberto, C. Gorse, A. Laricchiuta, P. Minelli, D. Pagano, *Physical Review E* **66** (2002) 016403

[26] M. Capitelli, R. Celiberto, C. Gorse, A. Laricchiuta, D. Pagano, P. Traversa, *Physical Review E* **69** (2004) 026412

[27] G. Singh and K. Singh, *Physics of Plasmas* **13** (2006) 122309

[28] B. Sourd, P. Andrè, J. Aubreton and M.F. Etchinger, *Plasma Chemistry and Plasma Processing* **27** (2007) 35

[29] B. Sourd, P. Andrè, J. Aubreton and M.F. Etchinger, *Plasma Chemistry and Plasma Processing* **27** (2007) 225

[30] D. Bruno, M. Capitelli, C. Catalfamo, A. Laricchiuta, "Cut-off Criteria of Electronic Partition Functions and Transport Properties of Atomic Hydrogen Thermal Plasmas" *Physics of Plasma* (2008) *in press*.

[31] R. Trampedach, W. Dappen, V.A. Baturin, *Astrophysical Journal* **646** (2006) 560

[32] F.J. Rogers, A. Nayfonov, *Astrophysical Journal* **576** (2002) 1064

[33] W. Dappen, L. Anderson, D. Mihalas, *Astrophysical Journal* **319** (1987) 195

[34] F.J. Rogers, F.J. Swenson, C.A. Iglesias, *Astrophysical Journal* **456** (1996) 902

[35] R.S. Devoto, *Physics of Fluids* **10** (1967) 2105

[36] M.Capitelli, *Journal of Plasma Physics* **7** (1972) 99

[37] J.M. Yos, *Revised Transport Properties for High Temperature Air and its components* AVC-RAD, (1967)

[38] J. Bacri, S. Raffanel, *Plasma Chemistry and Plasma Processing* **9** (1989) 133

[39] A.B. Murphy, *Plasma Chemistry and Plasma Processing* **15** (1995) 279

[40] M. Capitelli, C. Gorse, S. Longo, D. Giordano, *Journal of Thermophysics and Heat Transfer* **14** (2000) 259

[41] M.J. Wright, D. Bose, G.E. Palmer, E. Levin, *AIAA Journal* **43** (2005) 2558

[42] C. Nyeland, E.A. Mason, *Physics of Fluids* **10** (1967) 985

[43] M. Capitelli, E. Ficocelli, *Journal of Physics B* **5** (1972) 2066

[44] M. Capitelli, *Journal of Plasma Physics* **14** (1975) 365

[45] M. Capitelli, *Journal de Physique Supplement Colloque C3* (Paris) **38** (1977) 227

[46] A. Laricchiuta, D. Bruno, M. Capitelli, R. Celiberto, C. Gorse and G. Pintus, *Chemical Physics* **344** (2008) 13

[47] A. Eletskii, M. Capitelli, R. Celiberto, A. Laricchiuta, *Physical Review A* **69** (2004) 042718

[48] A.V. Kosarim, B.M. Smirnov, *Journal of Experimental and Theoretical Physics* **101** (2005) 611

[49] A.V. Kosarim, B.M. Smirnov, M. Capitelli, R. Celiberto, A. Laricchiuta, *Physical Review A* **74** (2006) 062707

[50] M. Capitelli, D. Cappelletti, G. Colonna, C. Gorse, A. Laricchiuta, G. Liuti, S. Longo, F. Pirani, *Chemical Physics* **338** (2007) 62

[51] F. Pirani, M. Albertí, A. Castro, M.M. Teixidor, D. Cappelletti, *Chemical Physics Letters* **394** (2004) 37

[52] F. Pirani, G.S. Maciel, D. Cappelletti, V. Aquilanti, *International Reviews in Physical Chemistry* **25** (2006) 165

[53] G. Liuti, F. Pirani, Chemical Physics Letters 122 (1985) 245

[54] R. Cambi, D. Cappelletti, G. Liuti, F. Pirani, Journal Chemical Physics 95 (1991) 1852

[55] F. Pirani, D. Cappelletti, G. Liuti, Chemical Physics Letters 350 (2001) 286

[56] D. Cappelletti, G. Liuti, F. Pirani, Chemical Physics Letters 183 (1991) 297

[57] V. Aquilanti, D. Cappelletti, F. Pirani, Chemical Physics 209 (1996) 299

[58] T. Miller, B. Bederson, *Advances in Atomic and Molecular Physics*, vol. **13**, (Eds. D.R. Bates & B. Bederson, Academic New York, 1977)

[59] R.K. Nesbet, *Physical Review A* **16** (1977) 1

[60] S. Fraga, K.M.S. Saxena, *Atomic Data* **4** (1972) 255

[61] A. Laricchiuta, G. Colonna, C. Gorse, R. Celiberto, F. Pirani, M. Capitelli, *Chemical Physics Letters* **445** (2007) 133

[62] A.B. Murphy, *Plasma Chemistry and Plasma Processing* **20** (2000) 279

[63] R.S. Devoto, *Physics of Fluids* **10** (1967) 354

[64] G. Hadinger, G. Hadinger, O. Bouty, M.A. Fr econ, *Physical Review A* **50** (1994) 1927

[65] M.I. Chibisov, R.K. Janev, *Physics Reports (Review Section of Physics Letters)* **166** (1988) 1

[66] A. Laricchiuta, D. Bruno, C. Catalfamo, F. Pirani, G. Colonna, P. Diomede, D. Pagano, C. Gorse, S. Longo, R. Celiberto, D. Giordano, M. Capitelli, AIAA Paper 2007-4043, 39th AIAA Thermophysics Conference, Miami, FL, June 25-28 2007

[67] G. Colonna, *Computer Physics Communications* **177** (2007) 493

[68] E. Eucken, *Physik Zeitschr* **14** (1913) 324

[69] J.H. Ferziger, H.G. Kaper, *Mathematical theory of transport processes in gases* (North-Holland, Amsterdam, 1972)

[70] E.A. Mason, L. Monchick, *Journal of Chemical Physics* **36** (1962) 1622

[71] C. Nyeland, G.D. Billing, *Journal of Physical Chemistry* **92** (1988) 1752

[72] E.V. Kustova, E. A. Nagnibeda, *Chemical Physics* **233** (1998) 57.

[73] R.S. Devoto, *Physics of Fluids* **9** (1966) 1230

[74] J.N. Butler, R.S. Brokaw, *Journal of Chemical Physics* **26** (1957) 1636

[75] M. Capitelli, *Z. Naturforsch. A* **29a** (1974) 953

[76] B.V. Alekseev, A. Chikhaoui, I.T. Grushin, *Physical Review E* **49** (1994) 2809

[77] W.E. Meador, L.D. Stanton, *Physics of Fluids* **8** (1965) 1694